Department of Environment Systems

Graduate School of Frontier Sciences

The University of Tokyo

2021

Master's Thesis

Assessment of Ecosystem Response in Pujada Bay by Water Quality Model Combined with Species Competition Model

Submitted August 19, 2021

Supervisor: Professor Shigure TABETA

李天野

Li Tianye

Contents

Chapter 1. Introduction

1.1 Background

Ecosystems are interacting, affecting others, and being affected by them. This is never more so underscored than in the coastal environment where, although the boundary between the terrestrial environment and the marine environment is clearly defined, the impacts are not. Land-based activities invariably affect the conditions of the coastal and marine environment just as the state of the coastal resources influence the activities on land. Anthropogenic activities impinge on coastal ecosystems through their adverse impacts on marine organisms residing at the bottom of the food chain; from there, the effects move up the food chain, magnifying the dire consequences especially in key bio resources such as algae and coral reefs.

In Philippines, the interrelatedness of adjacent ecosystems from rivers to estuaries down to coastal areas is exemplified in Pujada and Mayo Bays in Mati, Davao Oriental which is surrounded by forested, rugged mountain ranges and flatlands planted with a variety of agricultural crops. Pujada and Mayo Bays in southeastern Mindanao are important convergence points for the Pacific Ocean and Celebes Sea bioregions. While it is teeming with diverse biota and habitat, Pujada and Mayo Bays are also vulnerable to overexploitation and pollution from land-based activities.

To elucidate the type and volume of agrochemicals used in the surrounding areas as well as other pollutants that have leached into the bays to possibly cause marine pollution, this project named Development of a Comprehensive Coastal Ecosystem Modelling, Mapping and Monitoring Systems (CCEMMMS) is carried out in collaboration with the Davao Oriental State College of Science and Technology, Philippines. It is expected that the maps and models carried out by this project will be utilized as a spatial prioritization tool in identifying critical habitats and assigning appropriate zones within the two bays. It is also expected that they will be employed as a decision support tool for planning for the management of both bays as well as adjacent areas. With a system established for planning at the ecosystem level, ecosystem-based management is made more realistic. Management

interventions will be made with better predictions for future outcomes, ensuring that benefits ultimately redound to the community and that the environment is managed sustainably.

Against this background, the main part of this research is to make a physical-ecosystem model for understanding the current situation of water quality and its changing mechanism in Pujada Bay and try to develop a tool to assess the ecosystem response due to the water quality change.

1.2 Previous Research and Challenge

In the past numerous researches, many simulation models have been developed and applied to understand the various phenomena occurring in the marine environment. First, the physical simulation model plays a fundamental role to the material circulation in marine[1], whose development history is quite long. The Princeton Ocean Model[2] (POM), which was first developed, or the Regional Ocean Modeling System[3] (ROMS), which was improved from POM, these models are the very first members in the history of physical model development. Thereafter, the physical model diverged according to the simulation depth. As for the hydrodynamics in coastal seas, such as Stanford Unstructured Nonhydrostatic Terrain-following Adaptive Navier–Stokes Simulator[4] (SUNTANS) was carried out to simulate multiscale physics. With the attention given to the ecosystem, the simulation object of modelling has started to develop from physical simulation to ecosystem simulation. Some of the basic models, such as the Nutrient-Phytoplankton-Zooplankton-Detritus model[5] (NPZD), the PlankTOM model[6], or the North Pacific Ecosystem Model for Understanding Regional Oceanography[7] (NUMERO), all have a place in the development of ecosystem models. Further on, there were also models that emerged for the simulation of coral and algae[8,9].

Obviously, how to find and use a specific model based on requirements among a large number of models will become more difficult as the models continue to develop. Thus, the challenge now becomes how to combine the appropriate models for the purpose of the research, or whether a model with excellent scalability can be found that is compatible with various computational needs. This research was also but one part of a long process of exploration and proposed a feasible solution.

1.3 Objectives of This Research

This research has two main sections, reproduce the basic water quality and ocean current movement of the bay, and establish a rational link between human activities, water quality changes and ecosystem changes. In this research, a physical-ecosystem model, MEC Model (Marine Environmental Committee Model) is chosen as numerical model. MEC model is developed by Marin Environmental Committee, Society of Naval Architects of Japan. The simulation model has been developed over many years and MEC model is the one which has complete function and relative accuracy that is quite enough to be used for this research. By MEC Model, variables such as water temperature and salinity can be calculated, with the input of grid, river, climate, wind, and open boundary (including tide) data. The fundamental components of MEC Ocean Model are physical sub model and NPZF ecosystem sub model. Because physical disturbances play a vital role in nutrient diffusion and in sequence affects the distribution of aquatic living creatures, the former sub model is aimed to deal with the hydrodynamic conditions and water state. Then it is followed by a sub ecosystem model dealing with the chemical and biological features of research targets, which is a more direct index for environmental evaluation. After reproducing the water quality and ecological environment of Pujada Bay, a coral-algal competition model was introduced for the first time into the MEC model, which was used to predict the ecosystem trends under different conditions.

The structure of models used in this research is showed as Fig. 1.1.

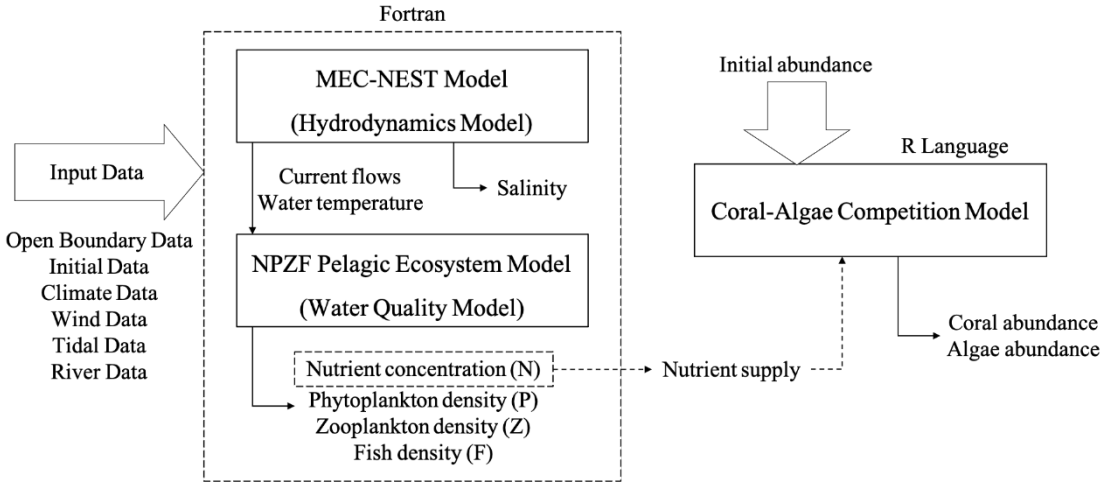

Fig. 1.1 Diagram of the models structure

The processes are broken down into following four steps:

- Collection and modification of relevant input data.
- Assume reasonable values for partial missing input data and conduct numerical simulations in Pujada Bay during certain time period to reproduce the environment.
- Introduce a coral-algae competition sub model to the water quality model.
- Based on the result of coupled model simulation, try to investigate the relevant response of ecosystem to human activities through scenario setting.

As a goal, this research is expected to be used to recommend adequate, practical, practicable, and crucial management interventions and to support conservation practices. We hope some results from this research can help to identify areas or factors that require the most urgent attentions and raise awareness among the coastal communities close to the affected areas about the real status of their coast to implement needed interventions.

Chapter 2. Hydrodynamics and Water Quality Model

2.1 Brief Introduction

The MEC Ocean Model was first proposed and developed by the Marine Environmental Committee of the Society of Naval Architects and Ocean Engineers of Japan, to numerically study the three-dimensional coastal hydrodynamics[10]. The prototype of MEC Model was Based on the model of multi-layer hydrodynamic simulation[11], tidal and meteorological effects were further integrated and validated[12]. By 2000, with the expanded exploitation of ocean space in Japan, e.g., artificial marine structures in Tokyo Bay, there existed a growing demand to evaluate the environmental effects of these marine structures[13]. To fulfill the new task, MEC model was planned and developed to be a suitable model.

Up to now, MEC Model has undergone a rapid development and been adopted in diverse fields. Basically, for the environmental investigation, MEC Model well performed in estuarine[14], inland sea[15], and lacustrine[16] environments. Further, when being coupled with other specific sub models, it has been proved as a useful tool for the design of marine structures, e.g., the density current generator[17] and the marine current turbine[18]; and similarly for the ocean space exploitation, e.g., sub-seafloor carbon storage strategy in Ardmuchnish Bay[19] and vessel speed trials around the Straits of Korea[20]. Not until recently, MEC Model began to shed light on the numerical study towards fishery activities, e.g., the impacts of fishing[21] and aquaculture[14].

2.2 Physical Sub Model

2.2.1 Introduction of MEC-NEST model

In the field of physical simulation, the common practice was conducted on the following components: tidal elevation, current flows, and water temperature as well as salinity. Generally, current flows are more readily affected by the external forces like tidal forces, wind frictions, the drag forces by aquaculture facilities, etc. The water temperature and salinity, although they are also affected by the

external fluctuations, show a smoother variation pattern than that of current flows, which also makes the prediction of water temperature/salinity easier than current flows from the theoretical perspective. Here MEC-NEST model was adopted to calculate the three-dimension seawater flow. It also can calculate tidal currents and advection-diffusion of substances.

2.2.2 Equations and transition processes

When the ocean is considered as an uncompressed viscous fluid, the behavior of the fluid is expressed by the following Navier-Stokes Equation.

$$\frac{D\vec{u}}{Dt} = \vec{K} - \frac{1}{\rho}\nabla p + \nabla^2\vec{u} \tag{2.1}$$

Where $\vec{u}$ is the viscosity; p is the pressure; ρ is fluid of density; $\vec{K}$ is body force; ∇ is Laplace operator.

The behavior of the fluid is calculated by solving this equation discretely. To simplify the calculation, the following approximation is used[12].

- Set an orthogonal coordinate system with x and y axis in horizontal direction and z axis in vertical downward direction.
- Except buoyancy part, the density is set as constant (Boussinesq approximation).
- Since the scale in the vertical direction is much smaller than the horizontal direction, the condition of no dynamic pressure in the vertical direction is assumed. The pressure of the fluid only considers the weight of seawater above (hydrostatic pressure approximation).
- Since the calculation area is small, it is approximated that there is no influence of the roundness of the earth, so the Cartesian coordinate system is used, and the Coriolis parameter is assumed to be constant (f-plane approximation).
- The process whose size are smaller than gird size is represented by the eddy diffusion term and the eddy viscosity term.
- Unstable thermal stratification is assumed that the sea water in upper layer and under layer intersect with each other instantaneously.
- The density of sea water is the function of temperature and salinity.

By these approximations, the equation of motion in the x, y, z direction and the continuous equations are listed as the following equations.

Continuity equation

$$\frac{\partial u}{\partial x}+\frac{\partial v}{\partial y}+\frac{\partial w}{\partial z}=0 \tag{2.2}$$

Motion equations (Full 3D model)

$$\frac{\partial u}{\partial t}+u\frac{\partial u}{\partial x}+v\frac{\partial u}{\partial y}+w\frac{\partial u}{\partial z}=-\frac{1}{\rho_0}\frac{\partial p}{\partial x}+f_v+A_M\left(\frac{\partial^2 u}{\partial x^2}+\frac{\partial^2 u}{\partial y^2}\right)+\frac{\partial}{\partial z}(K_M\frac{\partial u}{\partial z}) \tag{2.3}$$

$$\frac{\partial v}{\partial t}+u\frac{\partial v}{\partial x}+v\frac{\partial v}{\partial y}+w\frac{\partial v}{\partial z}=-\frac{1}{\rho_0}\frac{\partial p}{\partial y}-f_v+A_M\left(\frac{\partial^2 v}{\partial x^2}+\frac{\partial^2 v}{\partial y^2}\right)+\frac{\partial}{\partial z}\left(K_M\frac{\partial v}{\partial z}\right) \tag{2.4}$$

$$\frac{\partial w}{\partial t}+u\frac{\partial w}{\partial x}+v\frac{\partial w}{\partial y}+w\frac{\partial w}{\partial z}=-\frac{1}{\rho_0}\frac{\partial p}{\partial z}+f_v+A_M\left(\frac{\partial^2 w}{\partial x^2}+\frac{\partial^2 w}{\partial y^2}\right)+\frac{\partial}{\partial z}\left(K_M\frac{\partial w}{\partial z}\right)-\frac{\rho-\rho_0}{\rho_0}g \tag{2.5}$$

Motion equations (hydrostatic pressure approximation model)

$$\frac{\partial u}{\partial t}+u\frac{\partial u}{\partial x}+v\frac{\partial u}{\partial y}+w\frac{\partial u}{\partial z}=-\frac{1}{\rho_0}\frac{\partial p_s}{\partial x}+f_v+A_M\left(\frac{\partial^2 u}{\partial x^2}+\frac{\partial^2 u}{\partial y^2}\right)+\frac{\partial}{\partial z}(K_M\frac{\partial u}{\partial z}) \tag{2.6}$$

$$\frac{\partial v}{\partial t}+u\frac{\partial v}{\partial x}+v\frac{\partial v}{\partial y}+w\frac{\partial v}{\partial z}=-\frac{1}{\rho_0}\frac{\partial p_s}{\partial y}-f_v+A_M\left(\frac{\partial^2 v}{\partial x^2}+\frac{\partial^2 v}{\partial y^2}\right)+\frac{\partial}{\partial z}\left(K_M\frac{\partial v}{\partial z}\right) \tag{2.7}$$

$$0=-\frac{1}{\rho_0}\frac{\partial p_s}{\partial z}-g \tag{2.8}$$

Where t (s) means time; u, v, w (m/s) are the flow velocities in the x direction, y direction and z direction respectively. p_s (N/m^2) is hydrostatic pressure; the density of sea water is ρ (kg/m^3). The parameters above are state variables while the following ones are constant. Coriolis parameter is f_v (1/s); A_M, K_M (m/s) are the eddy viscosity coefficients in horizontal and vertical; g (m/s^2) is the acceleration of gravity and ρ_0 (kg/m^3) means the representative density of sea water. The Coriolis parameter is calculated using the latitude of a certain point ϕ (rad) and the rotation angular velocity Ω (rad/s).

$$f_v=2\Omega\sin\phi \tag{2.9}$$

In this model, the changes in water temperature, salinity, and ecosystem are also calculated, which could be solved by the following equations.

Advection-diffusion equations of the temperature and salinity

$$\frac{\partial T}{\partial t}+u\frac{\partial T}{\partial x}+v\frac{\partial T}{\partial y}+w\frac{\partial T}{\partial z}=A_c\left(\frac{\partial^2 T}{\partial x^2}+\frac{\partial^2 T}{\partial y^2}\right)+\frac{\partial}{\partial z}\left(\frac{K_c}{\sigma}\frac{\partial T}{\partial z}\right)+q_{TMP} \tag{2.10}$$

$$\frac{\partial S}{\partial t}+u\frac{\partial S}{\partial x}+v\frac{\partial S}{\partial y}+w\frac{\partial S}{\partial z}=A_c\left(\frac{\partial^2 S}{\partial x^2}+\frac{\partial^2 S}{\partial y^2}\right)+\frac{\partial}{\partial z}\left(\frac{K_c}{\sigma}\frac{\partial S}{\partial z}\right)+q_{SAL} \tag{2.11}$$

Density equation

$$\rho = \rho \cdot (p, T, S) \tag{2.12}$$

Where A_c, K_c is the horizontal and vertical eddy diffusivity coefficients, respectively. q_{TMP} and q_{SAL} represents the value that changes due to heat flux with the sea surface, evaporation of seawater, and precipitation. Equation $\rho=\rho \cdot (p,T,S)$ (*2.12*) is the state equation of the relationship between seawater density and water temperature, salinity. Also, the parameter of σ is definite as below.

$$\sigma = \begin{cases} 0 \; if \; \frac{\partial p}{\partial z} \geq 0 \\ 1 \; if \; \frac{\partial p}{\partial z} \leq 0 \end{cases} \tag{2.13}$$

Based on the above equations, the simulation of the water quality of a bay can be completed. In addition, the MEC-NEST model also allows us to change the resolution so the calculation can be carried out continuously from a wide area to specific area.

2.3 Ecosystem Sub Model

2.3.1 Introduction of NPZF pelagic ecosystem model

Although the depth span of Pujada Bay is very large in different areas (maximum depth over 1000 m), only the pelagic ecosystem is considered in this research because water depths over 400 m are neglected in the simulation and their environmental impact on the benthic ecosystem can be ignored. Meanwhile, due to the lack of in field observation data support, here a relatively simple ecosystem model which named NPZF pelagic ecosystem model was introduced. The structure of this model is shown in Fig. 2.1. The four main parameters in this model are: Nutrient concentration (N), Phytoplankton density (P), Zooplankton density (Z), and Fish density (F), note that the units of them are all mmol-N/m^3 and here the constant carbon of nitrogen ratio was set to 6.625 for the conversion of P and Z value.

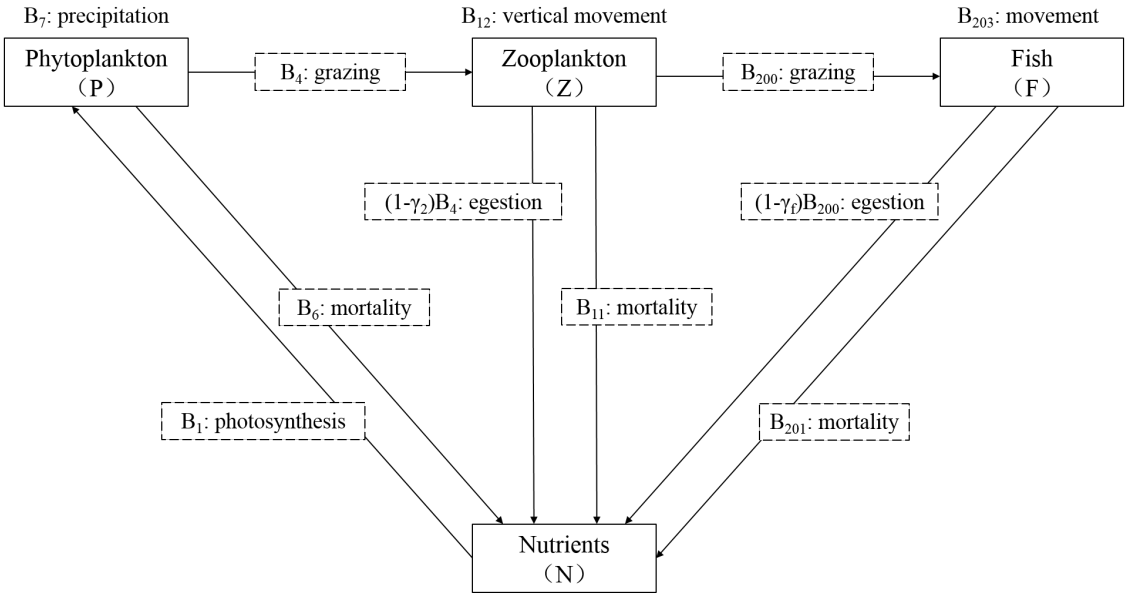

Fig. 2.1 The NPZF pelagic ecosystem model

2.3.2 Equations and transition processes

For this NPZF pelagic model, we assume that the organisms and substances considered are passive to the water flow. The change of each variable is calculated by the advection-diffusion equation shown in the following equation.

$$\frac{\partial B_i}{\partial t} + u\frac{\partial B_i}{\partial x} + v\frac{\partial B_i}{\partial y} + w\frac{\partial B_i}{\partial z} = A_c\left(\frac{\partial^2 B_i}{\partial x^2} + \frac{\partial^2 B_i}{\partial y^2}\right) + \frac{\partial}{\partial z}\left(K_c\frac{\partial B_i}{\partial z}\right) Q_{B_i} \tag{2.14}$$

where B_i is the variable concentration of each compartment in the ecosystem model, t is time. Besides, Q_{B_i} represents the time variation term of biological/chemical processes concerning each compartment, which are shown in the following equations.

Phytoplankton (PHY)

$$\frac{\partial PHY}{\partial t} = B_1 - B_4 - B_6 - B_7 \tag{2.15}$$

Zooplankton (ZOO)

$$\frac{\partial ZOO}{\partial t} = \gamma_z \cdot B_4 - B_{11} + B_{12} - B_{200} \tag{2.16}$$

Nutrient (NUT)

$$\frac{\partial NUT}{\partial t} = B_6 + B_{11} + B_{201} + (1-\gamma_z)\cdot B_4 + \left(1-\gamma_f\right)\cdot B_{200} \tag{2.17}$$

Fish density (FSH)

$$\frac{dFSH}{dt} = \gamma_f \cdot B_{200} - B_{201} + B_{203} \tag{2.18}$$

In these equations, the biological/chemical processes in the ecosystem model are shown in Table 2.1

Table 2.1 The biological/chemical processes in the ecosystem model

Symbol	Processes
B_1	Photosynthetic growth of phytoplankton
B_4	Phytoplankton grazing by zooplankton
B_6	Natural mortality of phytoplankton
B_7	Sinking of phytoplankton
B_{11}	Natural mortality of zooplankton
B_{12}	Vertical movement of zooplankton
B_{200}	Zooplankton grazing by fish
B_{201}	Natural mortality of fish
B_{203}	Migration of fish

The specific calculation of the biological/chemical processes are shown below.

Photosynthetic growth of PHY (B_1)

$$B_1 = \alpha_1 \cdot exp(\beta_1 T) \cdot \frac{NUT}{NUT+K_{NUT}} \cdot \frac{I}{I_{opt}} \cdot exp\left(1 - \frac{I}{I_{opt}}\right) \cdot PHY \tag{2.19}$$

Here, the light intensity I at a distance z from the water surface is given by the following equation according to Lambert-Beer's law.

$$I(z) = Q_r \cdot e^{-k_{ext} \cdot z} \tag{2.20}$$

$$Q_r = Q_{r_0} \cdot (1 - r) \tag{2.21}$$

where Q_r is the light intensity at the water surface, determined by the solar radiation amount Q_{r_0} and the reflectance of water surface r.

PHY grazing by ZOO (B_4)

$$B_4 = v_4 \cdot ZOO \tag{2.22}$$

$$v_4 = \alpha_4 \cdot exp(\beta_4 T) \cdot PHY \tag{2.23}$$

Natural mortality of PHY (B_6)

$$B_6 = \alpha_6 \cdot exp(\beta_6 T) \cdot PHY^2 \quad (2.24)$$

Sinking of PHY (B_7)

$$B_7 = \omega_{PHY} \frac{\partial PHY}{\partial z} \quad (2.25)$$

Natural mortality of ZOO (B_{11})

$$B_{11} = \alpha_{11} \cdot exp\ (\beta_{11} T) \cdot ZOO^2 \quad (2.26)$$

Vertical movement of ZOO (B_{12})

$$B_{12} = -\omega_{ZOO}(t) \frac{\partial ZOO}{\partial z} \quad (2.27)$$

$$\omega_{ZOO}(t) = -\omega_{down}\, sin\left(\frac{\pi}{DL} t\right) \quad \text{(Day)} \quad (2.28)$$

$$\omega_{ZOO}(t) = -\omega_{up}\, sin\left[\frac{\pi}{DL}(t - DL)\right] \quad \text{(Night)} \quad (2.29)$$

ZOO grazing by FSH (B_{200})

$$B_{200} = \alpha_{200} \cdot exp(\beta_{200} T) \cdot ZOO \quad (2.30)$$

Natural mortality of FSH (B_{201})

$$B_{201} = \alpha_{201} \cdot e^{\beta_{201} T} \cdot FSH \quad (2.31)$$

Migration of FSH (B_{203})

$$B_{203} = 0 \quad (2.32)$$

2.3.3 Parameters

In the numerical simulation of this research, the parameters of the ecosystem model were mainly based on previous research. After several test simulations, some of the parameters were adjusted to make the simulation results closer to the real situation in the Pujada Bay. The final values of parameters are shown in Table 2.2.

Table 2.2 Parameters in the ecosystem model

Symbol	Parameter	Value	Unit
γ_z	Assimilation efficiency of ZOO	0.7	-
γ_f	Assimilation efficiency of FSH	0.7	-
α_1	Maximum growth rate of PHY at 0℃	1.04×10^{-5}	1/s
β_1	Temperature effect for α_1	6.33×10^{-2}	1/℃
I_{opt}	Optimum light intensity for photosynthesis	97	$J/m^2/s$
K_{NUT}	Half saturation constant for NO_3 uptake of PHY	21	mmol N/m^3
k_{ext}	Extinction coefficient of light	0.8	-
α_4	Maximum PHY grazing rate of ZOO at 0℃	2.08×10^{-8}	1/s
β_4	Temperature effect for α_4	6.93×10^{-2}	1/℃
α_6	Natural mortality rate of PHY at 0℃	8.68×10^{-12}	$m^3/s/mmol\text{-}N$
β_6	Temperature effect for α_6	0	1/℃
ω_{PHY}	Sinking velocity of PHY	2.0×10^{-6}	m/s
α_{11}	Natural mortality rate of ZOO at 0℃	1.08×10^{-6}	$m^3/s/mmol\text{-}N$
β_{11}	Temperature effect for α_{11}	0	1/℃
α_{200}	Maximum ZOO grazing rate of FSH at 0℃	2.08×10^{-6}	1/s
β_{200}	Temperature effect for α_{200}	6.93×10^{-2}	1/℃
α_{201}	Natural mortality rate of FSH at 0℃	1.16×10^{-8}	$m^3/s/mmol\text{-}N$
β_{201}	Temperature effect for α_{201}	0	1/℃
$[Chl.a:N]_{PHY}$	Weight ratio of Chlorophyll-a to N of PHY	0.139	-

Chapter 3. Coral-Algae Competition Model

3.1 Brief Introduction

Coral-algae model was introduced to MEC-NEST model in this research to accurately capture the key dynamics structuring real reefs in the Pujada Bay region. Traditionally, the large-scale or long-term manipulative experiments that have been considered necessary[22] or the more recent variance-based approaches[23] usually require data at impractically high resolution for many ecological systems. Predicting the specific thresholds that produce shifts in natural systems remains a challenge[24], but by developing strategies to quantify feedbacks, a new tool is proposed to help address this challenge. The strategy used by this competition model could be employed in other systems without the need for manipulative experiments or long-term monitoring of community composition[22,25], which also provides a research convenience to the current lack of field data. By quantifying spatial patterns of herbivory and algal growth rates, this model was able to identify feedback processes and evaluate their impact at the whole reef scale. Modelling complex systems like coral reefs is inherently imperfect, it can be never certain that model conclusions will map onto real-world systems, but this model offer an approach to scale up local empirical data to draw solid, evidence-based insights into the workings of real systems, which can also be broadly applicable. It means that combined modelling and empirical approach can be generalized to any ecosystem where the existing community modifies environmental conditions or changes access to resources, thereby shifting competitive outcomes. The rapid nature of this model and the fact that it does not require destructive manipulations makes it particularly effective for systems of conservation concern.

3.2 Model Materials and Methods

3.2.1 Model structure

The coral-algae competition model is a stochastic cellular automaton model using the R programming language to evaluate the dynamics of coral and algal competition for space under varying environmental conditions[26]. This model also consists of a set of grids, and the main benthic community member that occupying the grid defines the stage it is in. The major benthic community members on the study reefs were live coral, macroalgae, and a mixed community of crustose coralline algae (CCA) and turf algae[27], and they are used as states in this model. It should be mentioned that two macroalgal states are included which represent newly colonized patches (M_1) and patches that persisted for multiple time steps (M_2). This distinction is included due to the most common mechanism for coral mortality that used to be observed was overgrowth and eventual smothering by macroalgae[28]. By incorporating separate phases, it was able to distinguish between coral that had recently been overgrown and could recover to the live coral state (L) when the macroalgae was removed and patches that had undergone coral mortality and would transition to the turf/CCA state (T). The complete model structure is shown in the Fig. 3.1.

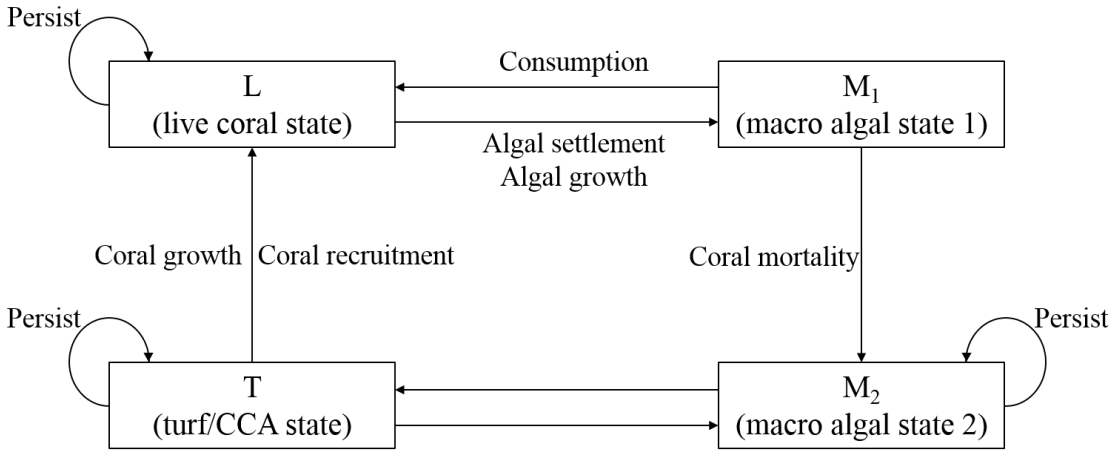

Fig. 3.1 The coral-algae competition model[25]

3.2.2 Equations and transition processes

Environmental conditions are usually constant throughout the landscape range, which is determined by the parameters of global nutrient supply (n) and herbivory potential (h). In this model, however, feedback processes in local communities could modify these conditions, so local nutrient supply (N) and herbivory pressure (H) for each cell need to be taken into consideration. Since both feedback processes are spatially localized, their effects are determined by the abundance of coral and algae in the local neighborhood (respectively as L_c and L_a).

Nutrients released from algae diffuse across the reef but are taken up very quickly, so the facilitative effect of algae on nutrient levels decays with distance. Thus, the nutrient facilitation neighborhood of a given cell is calculated as the weighted proportion of neighboring cells that are occupied by algae (of any type M_1, M_2, or T), with weights decreasing as the square of distance out to a maximum nutrient facilitation distance d_n. The model treats distance as a series of concentric rings out from the focal cell, and cells within a ring are equivalent whether they are vertically, horizontally or diagonally connected. So, the abundance of algae is calculated according to the following equation.

Abundance of algae

$$L_a = \sum_{i=1}^{d_n} \frac{x_i}{i^2} / \sum_{i=1}^{d_n} \frac{1}{i^2} \tag{3.1}$$

where x_i is the proportion of cells in the i^{th} ring of cells out from the focal cell that is occupied by any type of algae. The denominator serves to normalize the weighted mean calculation so that L_a can range from 0 to 1. In contrast to nutrient facilitation, herbivores exhibiting spatial fidelity have been shown to consume algae up to a fixed distance from coral refuges, rather than reducing herbivory pressure with distance from coral[29,30]. To reflect this pattern, the coral abundance (L_c) in the coral facilitation neighborhood is calculated simply as the overall proportion of coral cells within all the rings out to the herbivory facilitation distance (d_h).

Local nutrient supply (N) is dependent on global nutrient supply (n) modified by nearby algae that increase local nutrient availability via fixation and recycling. n also sets a base level for nutrient availability is enriched by an amount assumed to be linearly proportional to La with constant of proportionality y due to the assumption that all algae have equivalent facilitation abilities. The specific calculation equation is as follow.

Local nutrient supply

$$N = n(1 + yL_a) \tag{3.2}$$

Similarly, the maximum value of local herbivory pressure (H) is controlled by the herbivory potential (h) in the whole system, but here it is also necessary to consider that in real situation there is a fraction of herbivores *f* with spatial fidelity that do not range far away from coral refuges, then the herbivory pressure of a given cell should be lower. In this model, herbivores are assumed to be distributed throughout the landscape, but those with spatial fidelity will concentrate their algal consumption in areas with more corals. As a result, the herbivory pressure can be described by the following equation.

Local herbivory pressure

$$H = h(1 - f + fL_c) \tag{3.3}$$

where the activity of high-fidelity herbivores is proportional to the abundance of nearby coral (L_c) that provide refugia.

Assuming that local herbivory pressure and nutrient supply are linearly proportional to coral and algal abundance, respectively, is a simplifying approach. In order to make patch- and population-level dynamics of corals and algae respond nonlinearly to environmental conditions and thus follow a more biologically consistent pattern than would occur with negative or infinitely high algal growth rates, the model limits the range of other parameters in the analysis. These quantities inform process rates in conjunction with other parameters and actual transitions in the model are governed by probabilities that incorporate the rates via a saturating function. Related information will be mentioned later.

There are six processes drive transitions between states in this model. Five occur as Poisson processes with probabilities determined by local environmental conditions and community composition, which are shown in Table 3.1. The sixth process, coral mortality caused by macroalgae, occurs only for cells in the M_1 state and a transition to the M_2 that reflecting death of the underlying coral state always occurs if the macroalgae are not consumed in a 2-week time step.

Table 3.1 The transition processes in the competition model

Symbol	Processes
L_a	Abundance of algae
L_c	Abundance of coral
N	Local nutrient supply
H	Local herbivory pressure
λ_h	Macroalgal consumption rate
λ_a	Macroalgal growth rate
λ_p	New algal propagules settlement rate
λ_r	New coral colonies recruitment rate
λ_c	Coral growth rate
A_c	Directly adjacent coral
A_a	Directly adjacent algae

Rates for each process were calculated using the local environmental variables (*H, N*), local community composition (L_c, L_a), parameters for the rates of dispersal of coral and algae into the system and scaling coefficients for each process (σ_i). Scaling coefficients did not influence the behavior of the model, but they allowed the model to reflect natural rates for different systems. The specific calculations are as follows.

Macroalgal consumption rate

$$\lambda_h = \sigma_h H \tag{3.4}$$

Macroalgal growth rate

$$\lambda_a = \sigma_a N(1 - H) \tag{3.5}$$

New algal propagules settlement rate

$$\lambda_p = \sigma_p p N(1 - H) \tag{3.6}$$

Where p is the supply of algal propagules.

New coral colonies recruitment rate

$$\lambda_r = \sigma_r r \tag{3.7}$$

Where r is a single empirically estimated parameter of supply of coral recruits.

Coral growth rate (λ_c)

$$\lambda_c = \sigma_c L_c \tag{3.8}$$

Using these average rates, probabilities for each transition were calculated for each cell at each time step using a standard exponential formulation for Poisson processes.

$$P(Transition) = 1 - e^{-\lambda A \Delta t} \tag{3.9}$$

Where A is the number of directly adjacent coral (A_c) or macroalgae (A_a) cells.

Using this formulation with the rate expressions for each individual process probabilities can be calculated at every location for each time as follows.

$$P(consumption) = 1 - e^{-\sigma_h H \Delta t} \tag{3.10}$$

$$P(algal\ growth) = 1 - e^{-\sigma_a N(1-H) A_a \Delta t} \tag{3.11}$$

$$P(algal\ settlement) = 1 - e^{-\sigma_p N(1-H) \Delta t} \tag{3.12}$$

$$P(coral\ recruitment) = 1 - e^{-\sigma_r r \Delta t} \tag{3.13}$$

$$P(coral\ growth) = 1 - e^{-\sigma_c L_c A_c \Delta t} \tag{3.14}$$

Where negative values are treated as a probability of 0.

3.2.3 Parameters

In this model, several parameters are taken as a range. Due to the lack of field data, this method is used to make the simulation results closer to the real situation by adjusting them in real time. Among them, values for the scaling factors σ_h, σ_a, σ_r and σ_c based on 4 experiments[26,27,31,32]. Since there were no conditions to conduct the relevant experiments at the time of this research, the data from other research were directly used here. Specific values are shown in Table 3.2.

Table 3.2 Parameters in the coral-algae competition model

Symbol	Parameter	Value
h	Herbivory potential	0-2
n	Global nutrient supply	0-1
y	Efficiency of algal nutrient cycling	0-8
f	Herbivore spatial fidelity	0-1
d_n	Nutrient facilitation distance	1
d_h	Herbivory facilitation distance	1
p	Algal propagule supply	0.01
r	Coral recruit supply	0.01
σ_h	Consumption scaling factor	1.386
σ_a	Algal growth scaling factor	0.288
σ_p	Algal settlement scaling factor	1
σ_c	Coral growth scaling factor	0.257
σ_r	Coral recruitment scaling factor	1

Chapter 4. Bay Environment and Computational Condition

4.1 Basic Information on Pujada Bay

Pujada Bay is a U-shaped bay with an opening that faces towards the south-southeast and small islands are found at its mouth (Fig. 4.1). It has several freshwater tributaries (Magum River, Matiao Creek and Pahamutang Creek). It encloses an area of 168 square km shared by 10 coastal barangays of Mati, Davao Oriental. Bathymetry for Pujada Bay has been processed by Philippines side. Due to the patchy data from the sampling stations, bathymetric data from the sampling were combined with Global Multi-Resolution Topography (GMRT), a synthesis of in situ, model and satellite data.

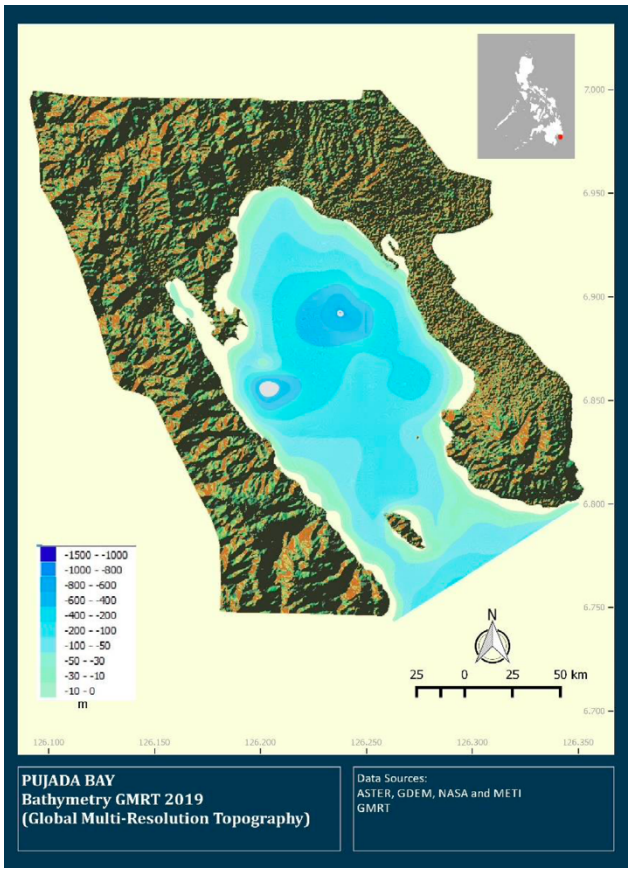

Fig. 4.1 Map of Pujada Bay bathymetry

4.2 Computational Condition

4.2.1 Simulation area

The simulation area was a rectangle range between 6.74~6.98°N and 126.14~126.35°E, with 30-degree rotation. The only open boundary was located at the lower side of this area, and the whole area was divided into 200m-size meshes (66×115) horizontally. The grid data is shown as Fig. 4.2.The three marked points are local observation sites, which are located at the mouths of the rivers entering the bay (respectively near Magum River, Matiao Creek and Pahamutang Creek), so these three positions were also used to locate the river outlets.

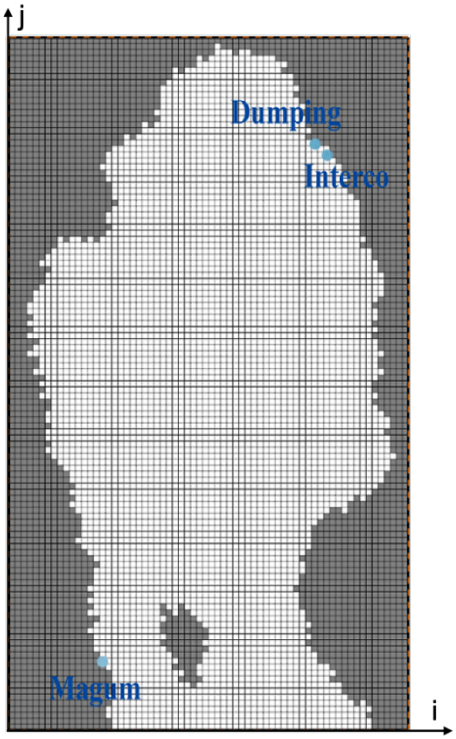

Fig. 4.2 Grid map for simulation

In vertical direction, the area was divided into 31 layers as Table 4.1. Considering that currents near the ocean surface are more influenced by meteorological factors such as wind and solar heat, the layers near the surface were divided more compactly. As mentioned above, the depth variation of Pujada Bay is very large, but considering that the deep sea is less affected by human activities and will reduce the stability of the model simulation, the part with depths greater than 400m was ignored. The grids at the

edge of the shoreline were also finely adjusted for the MEC-NEST model by ignoring or unifying the depth of some grids that are too shallow.

Table 4.1 The vertical division of simulation area

Layer Number	Depth	Thickness	Layer Number	Depth	Thickness
1	-4~-2m	2m	17	28~30m	2m
2	-2~0m	2m	18	30~35m	5m
3	0~2m	2m	19	35~40m	5m
4	2~4m	2m	20	40~45m	5m
5	4~6m	2m	21	45~50m	5m
6	6~8m	2m	22	50~60m	10m
7	8~10m	2m	23	60~70m	10m
8	10~12m	2m	24	70~80m	10m
9	12~14m	2m	25	80~90m	10m
10	14~16m	2m	26	90~100m	10m
11	16~18m	2m	27	100~150m	50m
12	18~20m	2m	28	150~200m	50m
13	20~22m	2m	29	200~250m	50m
14	22~24m	2m	30	250~300m	50m
15	24~26m	2m	31	300~400m	100m
16	26~28m	2m			

4.2.2 Calculation of time step

CFL Condition (Courant-Friedrichs-Lewy Condition) is used to calculate the time step by the following equation. Explanations of symbols in CFL Condition is in Table 4.2.

Time step

$$\Delta t \leq \frac{\Delta x}{\sqrt{2gh_{max}}} \tag{4.1}$$

Table 4.2 Explanations of symbols in CFL Condition

Symbol	Meaning	Unit
Δt	Time step	s
Δx	The length of each grid	m
g	Acceleration of gravity	m/s^2
h_{max}	The maximum depth	m

Due to the length of grid was 200 m and the h_{max} was 400 m, the time step should be $\Delta t \leq 2.26$ (s). In this research, the time step was set as 2 seconds.

4.2.3 Simulation period

Pujada Bay is in a region where climate change is not very significant throughout the year, and where there is a lack of field data to support. Considering the stability and comparability of the simulation，two separate time periods were simulated in this research, July 1 to July 30 in 2020 (wet season), and September 1 to 30 in the same year (dry season).

4.3 Input Data and Related Adjustment

The various data involved in this research were partly obtained from reports of the Davao Oriental State College of Science and Technology, Philippines. Parts of the missing data were filled in via the Internet.

4.3.1 Climate data

Atmospheric temperature, atmospheric pressure, amount of global solar radiation, cloud amount, relative humidity and precipitation are needed in the simulation of MEC-NEST model. All data were from CMEMS[33] and SOLCAST[34]. Variables included in the climate data are shown in Table 4.3.

Table 4.3 The variables included in the climate data

Variables	Unit
Atmospheric Temperature	℃
Atmospheric Pressure	hPa
Amount of Global Solar Radiation	$J/m^2/s$
Cloud Amount	-
Relative Humidity	-
Precipitation	mm/s

Input climate data are shown as the following figures. It should be noted that only the daily total rainfall was available for the precipitation data, so the precipitation per second input here was based on the daily total rainfall by converting them into average distribution over certain hours.

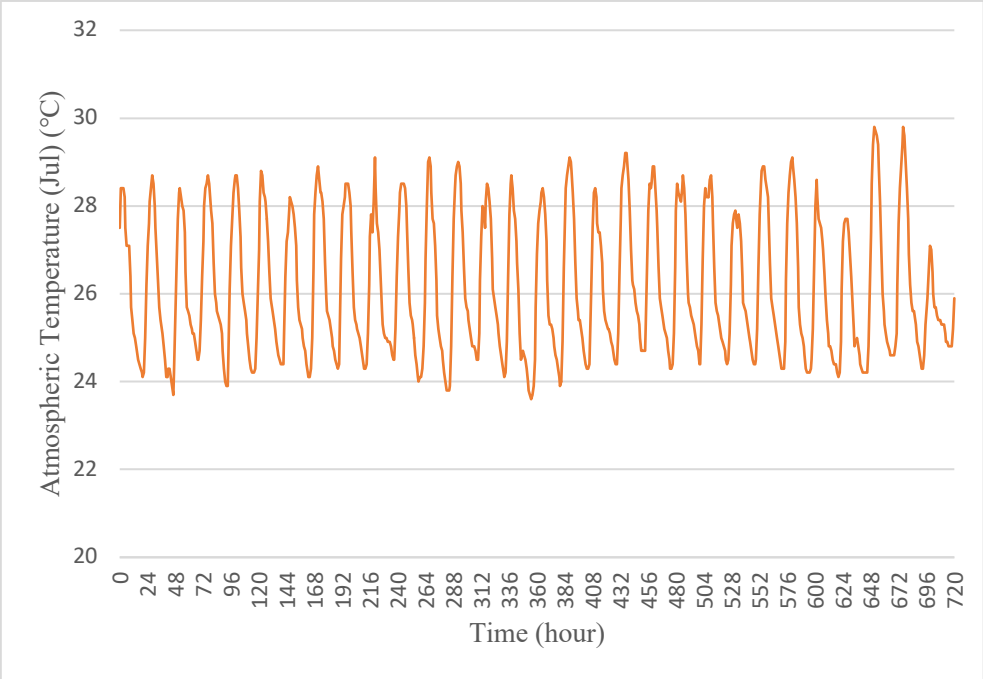

Fig. 4.3 Input data of atmospheric temperature (July)

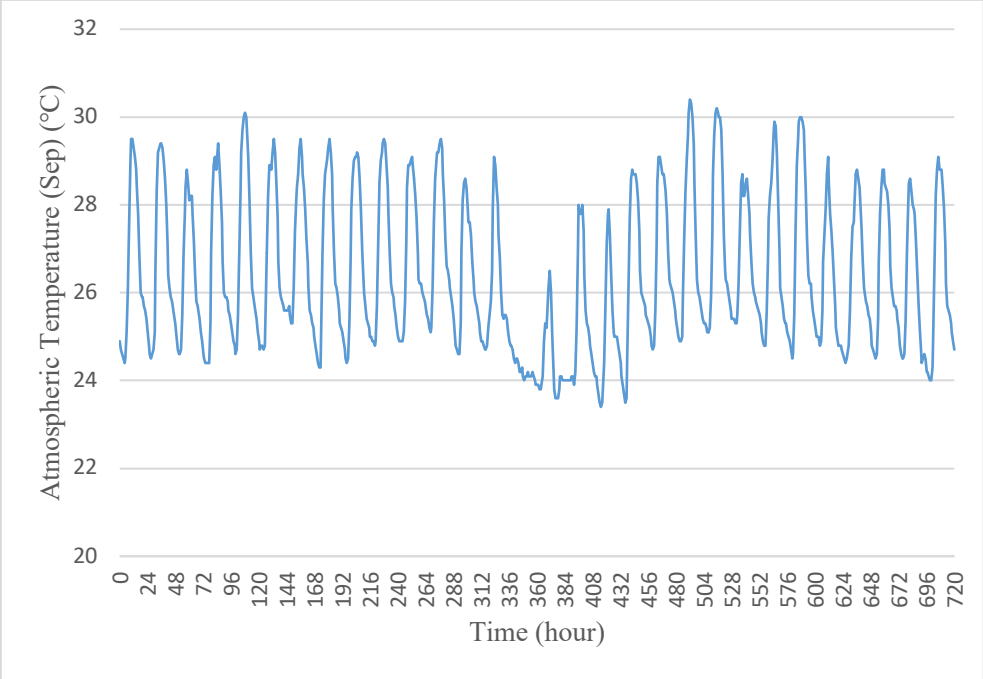

Fig. 4.4 Input data of atmospheric temperature (September)

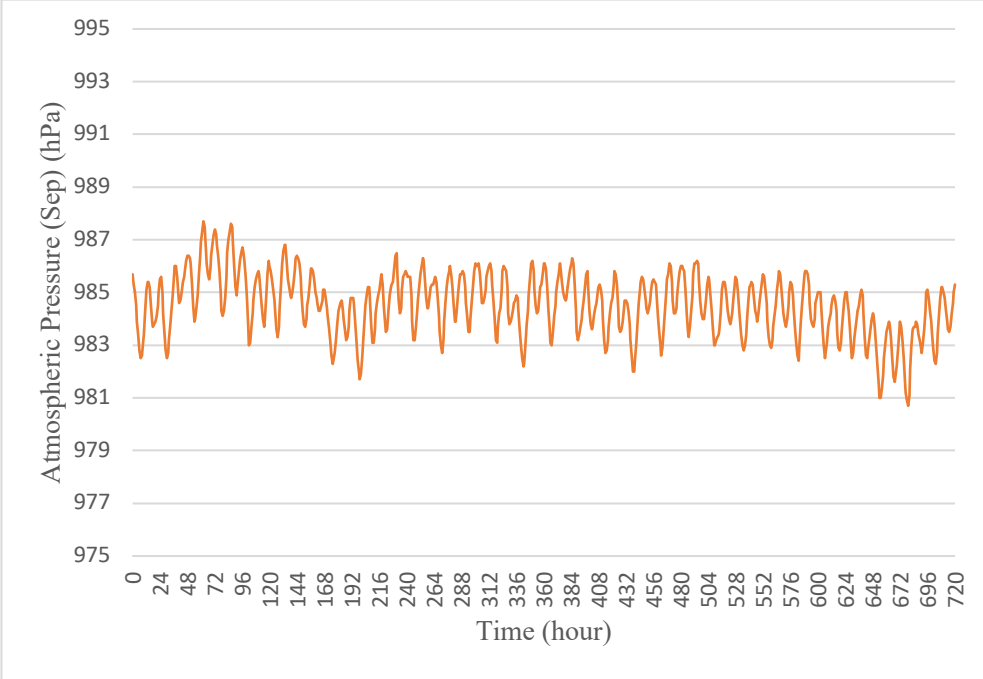

Fig. 4.5 Input data of atmospheric pressure (July)

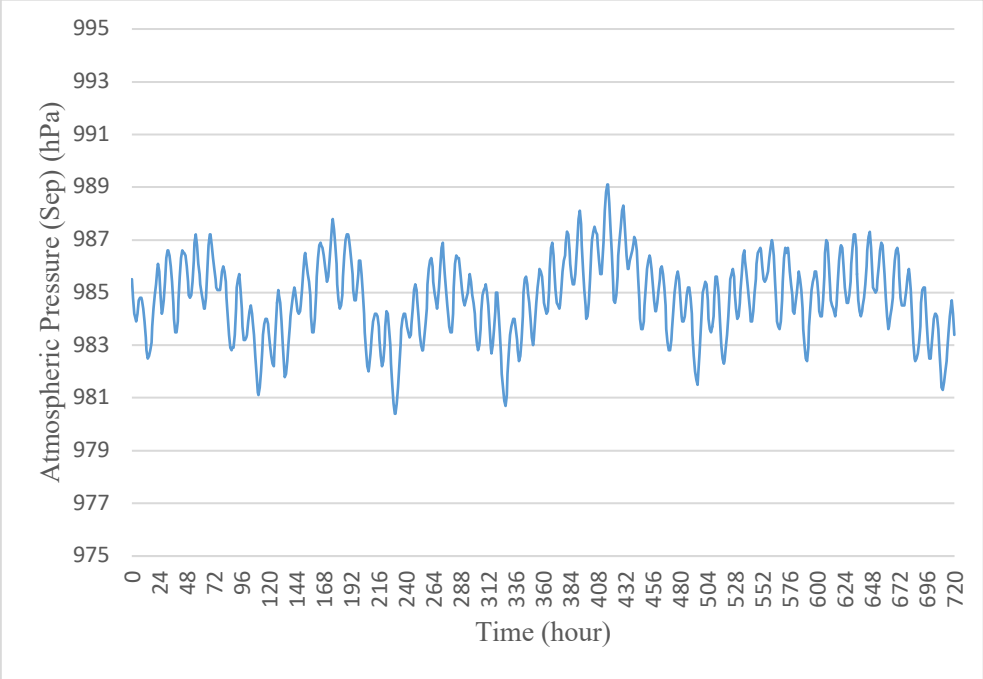

Fig. 4.6 Input data of atmospheric pressure (September)

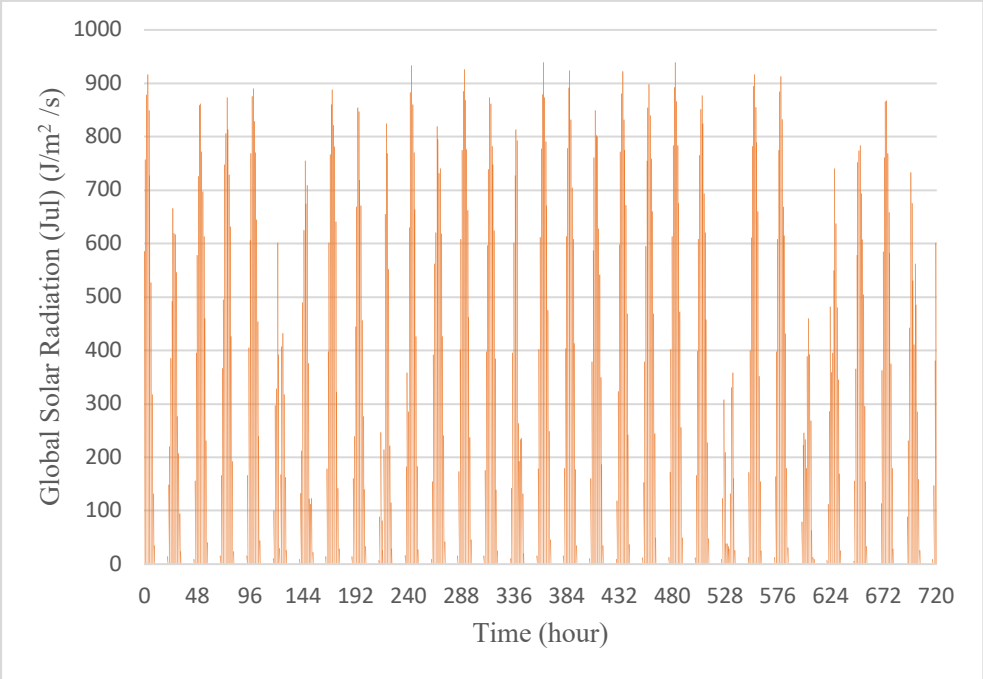

Fig. 4.7 Input data of amount of global solar radiation (July)

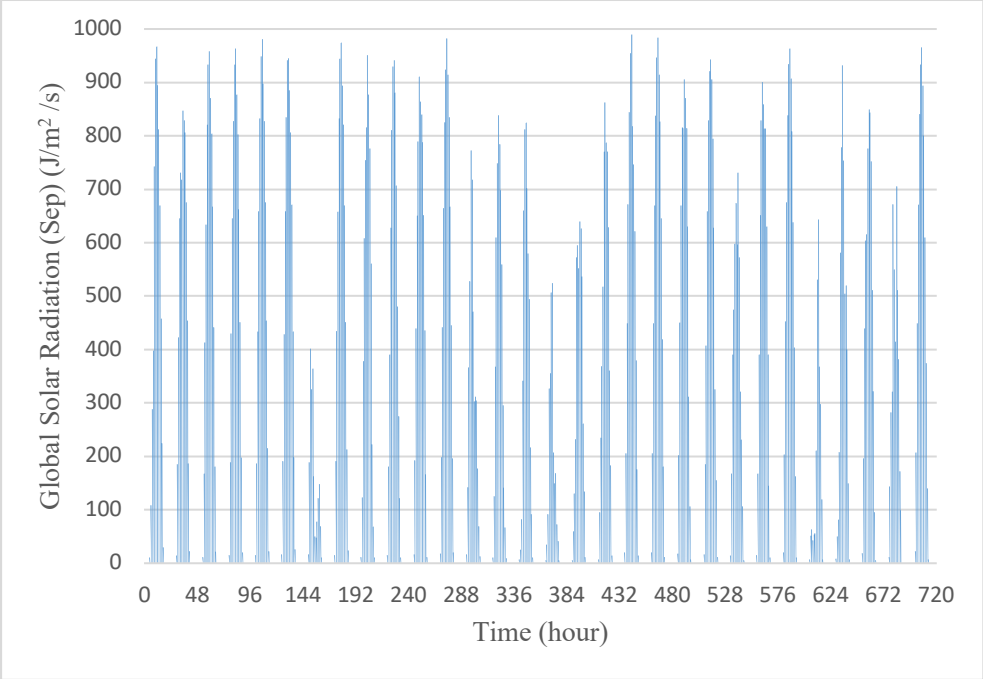

Fig. 4.8 Input data of amount of global solar radiation (September)

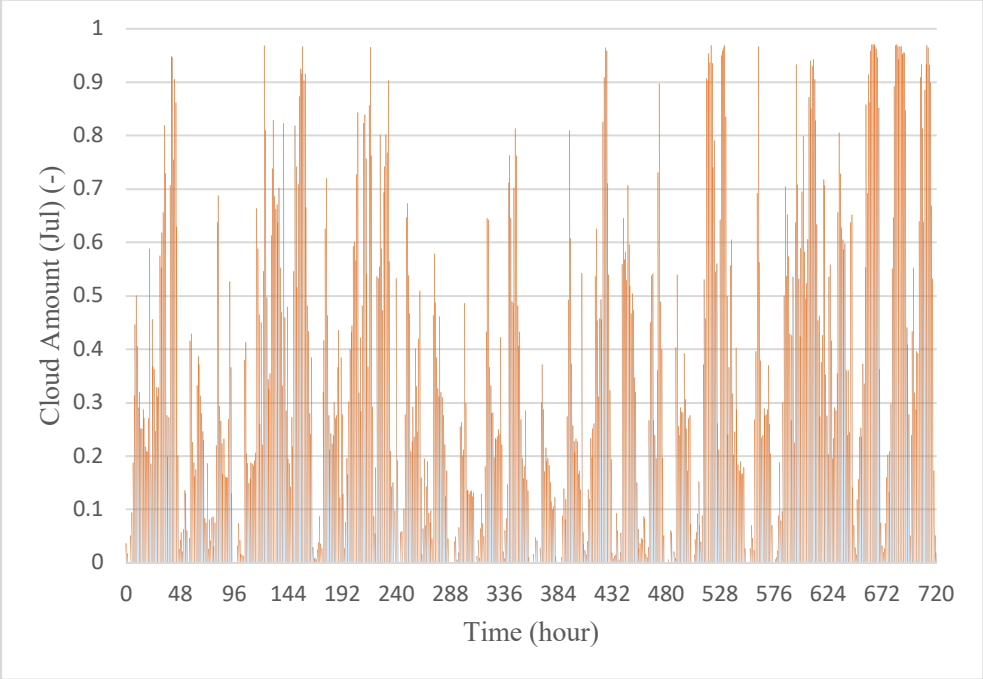

Fig. 4.9 Input data of cloud amount (July)

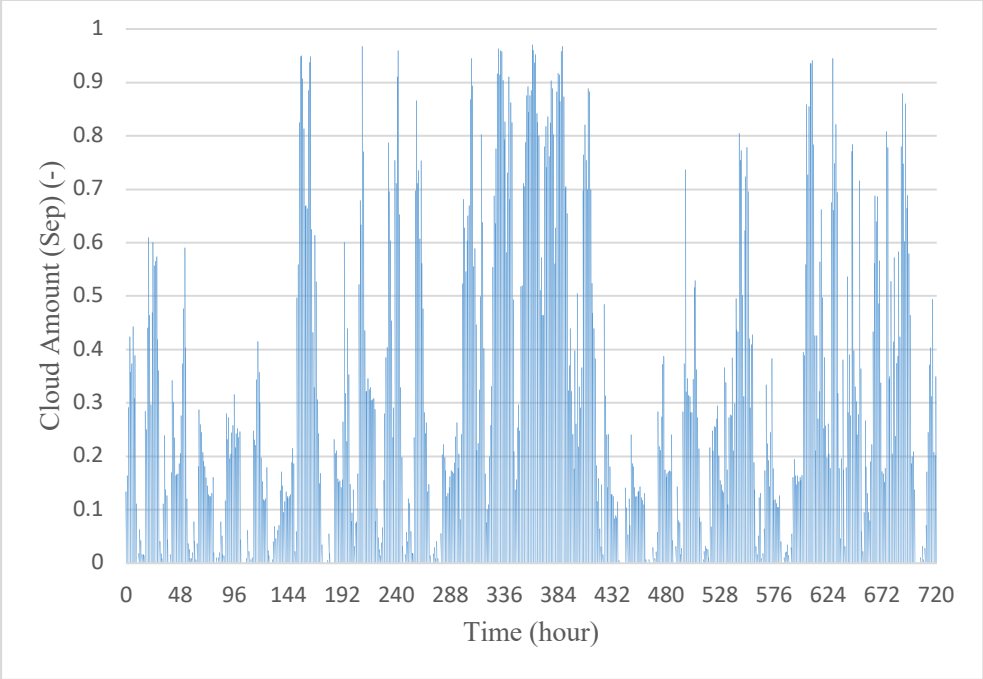

Fig. 4.10 Input data of cloud amount (September)

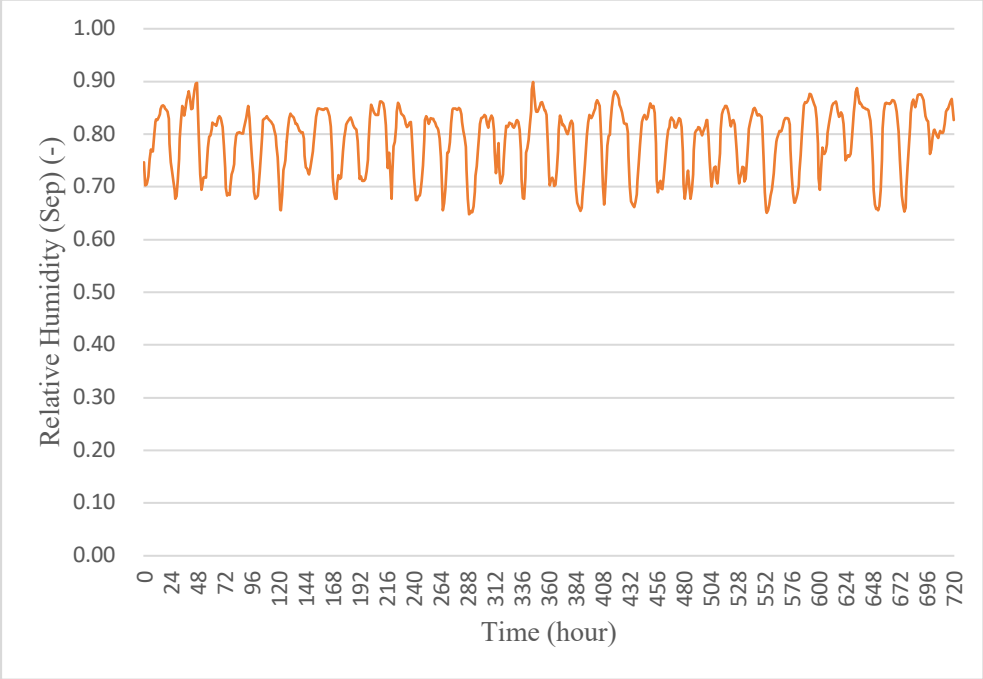

Fig. 4.11 Input data of relative humidity (July)

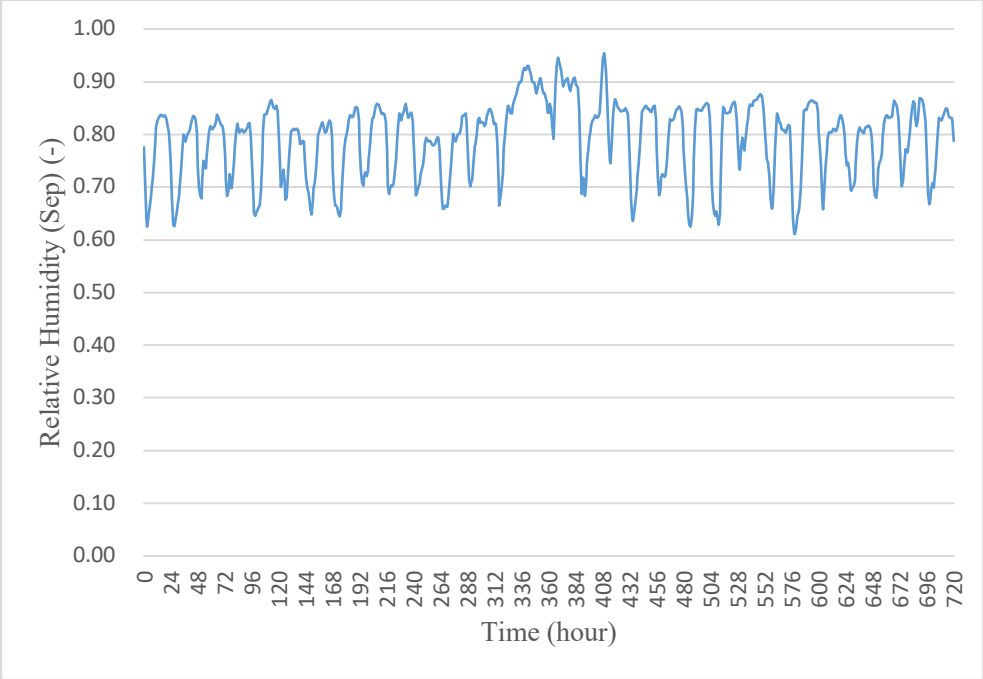

Fig. 4.12 Input data of relative humidity (September)

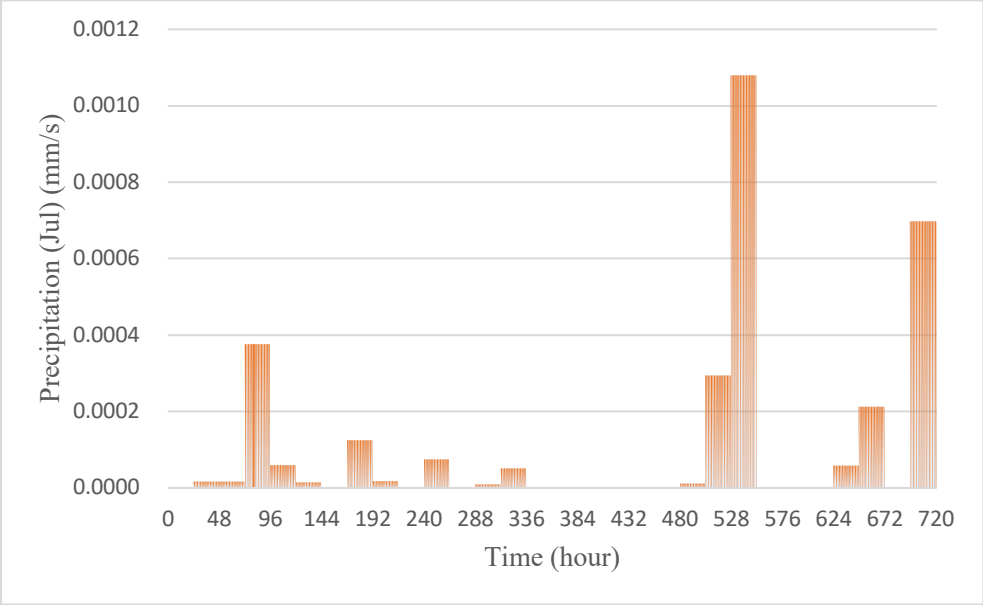

Fig. 4.13 Input data of precipitation (July)

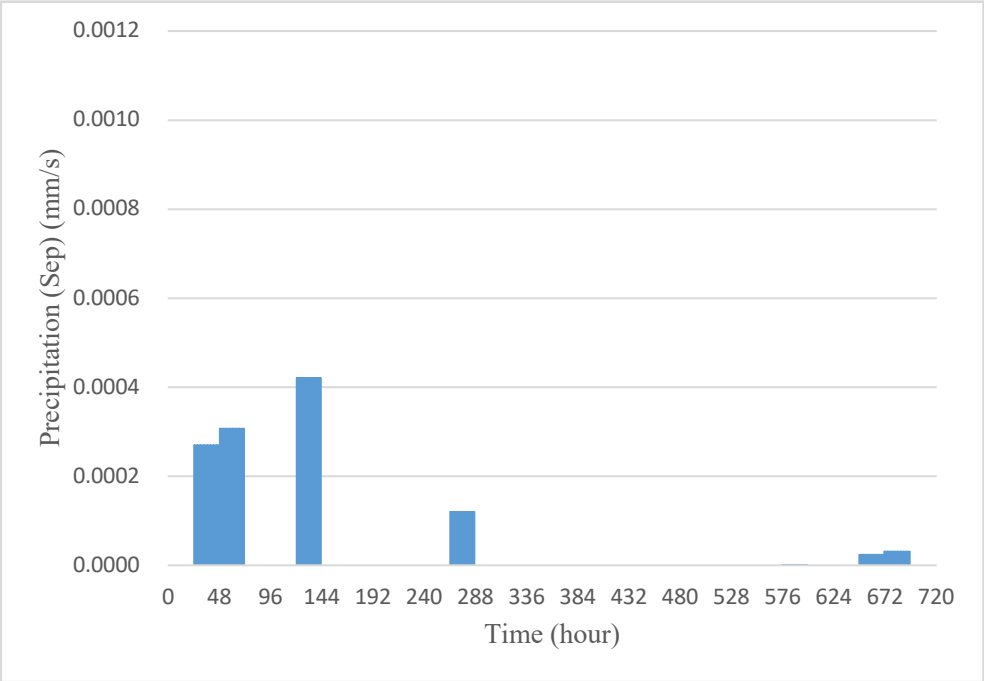

Fig. 4.14 Input data of precipitation (September)

4.3.2 Wind data

Input data of wind speed are required to be decomposed orthogonally into speed component toward north and speed component toward east in the MEC-NEST model. Wind data were from CMEMS[33]. The observation site of the wind data is in the southwest corner of the bay, and since no other more observation sites exist, the data measured at this site was considered as the wind data of the whole bay. Wind speed component toward north and east are shown in Fig. 4.15 to Fig. 4.18.

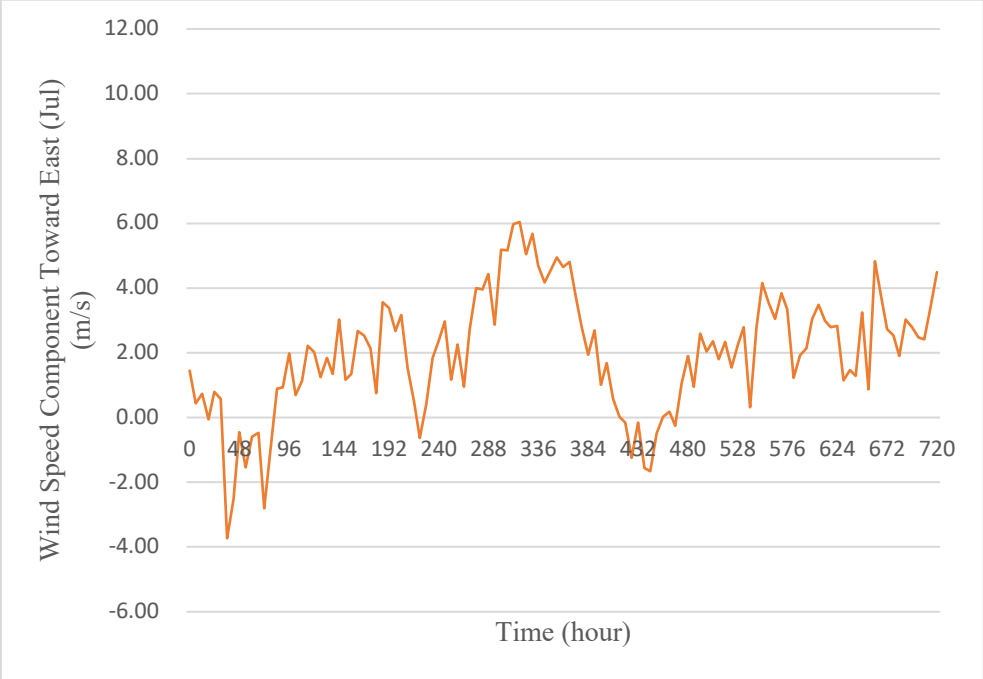

Fig. 4.15 Input data of wind speed component toward east (July)

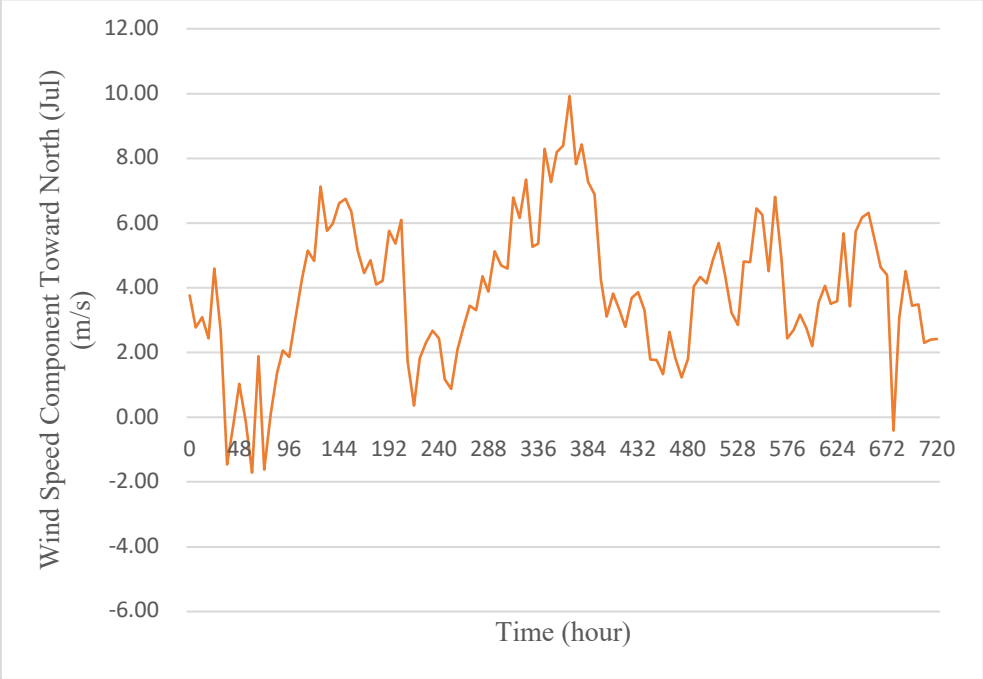

Fig. 4.16 Input data of wind speed component toward north (July)

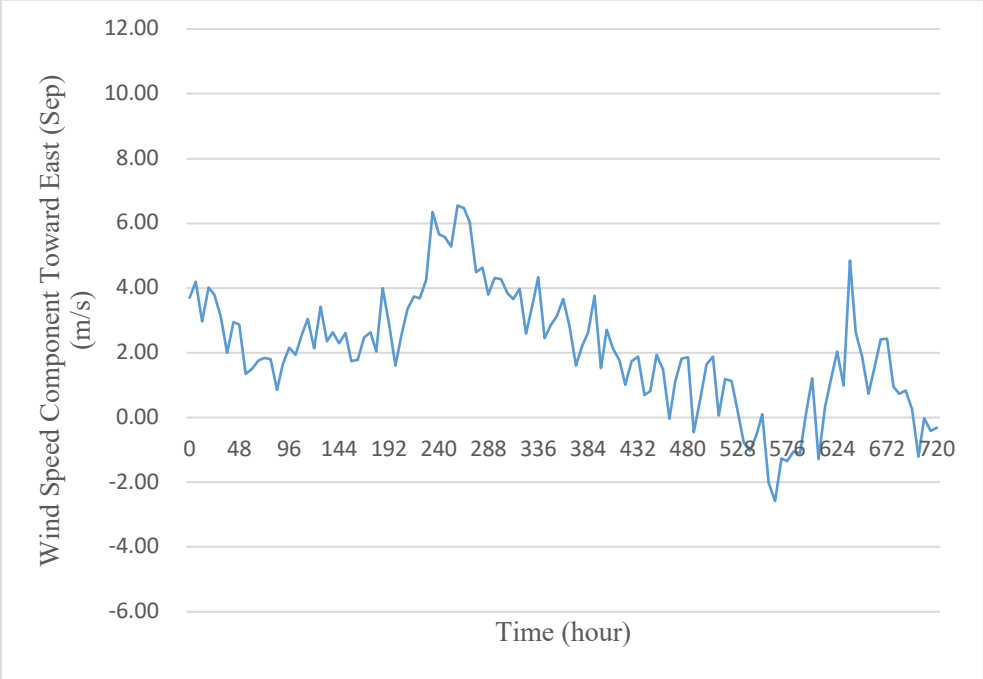

Fig. 4.17 Input data of wind speed component toward east (September)

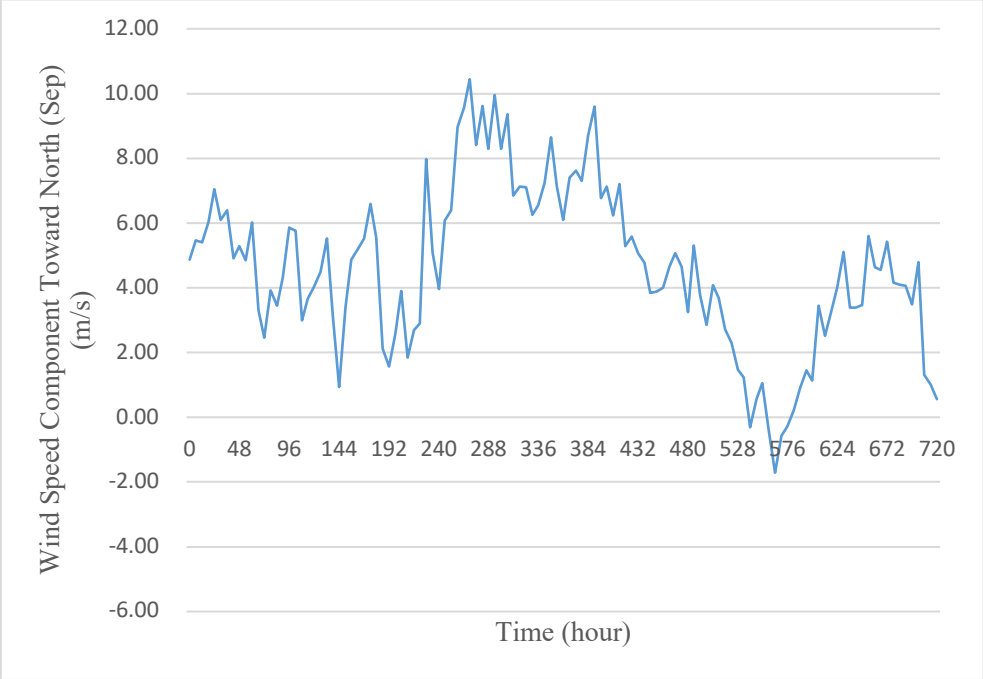

Fig. 4.18 Input data of wind speed component toward north (Spetember)

4.3.3 Open boundary data

Tidal data

In this research, although relevant tidal data could be found, the MEC-NEST model requires different constituents to simulate the real tidal environment. These constants and associated values are not directly available at present, so a simple method of only backpropagating the Principal Lunar Semi-Diurnal Tide from observation data was used in this research, and the resulting simulated tides will deviate significantly from the real situation but will not have much impact for the purpose of this research. Historical tidal data was obtained from TIDES4FISHING[35]. Details of the constituents at Mati that were used in the model can be referred to in Table 4.4.

Table 4.4 The information of tide at Mati

Location	Constituent	Symbol	Period (s)	Amplitude (m)
MATI, Davao Oriental (06°57′N, 126°13′E)	Principal Lunar Semi-Diurnal Tide	M2	44714.164	1.30

Water quality data

Except for the tidal data, Water quality data of the open sea (water temperature, salinity, phytoplankton, zooplankton, nutrient, fish density) are also required by the MEC-NEST model. For these input data, the observation data from an out-of-bay observation site were used because it is the nearest site from the open sea. The location information is shown in Table 4.5. To make the final simulation results closer to the real situation, four moments of open boundary data were used in this study, which were day 1, day 10, day 20 and day 30. It should be added that input data of zooplankton was based on the ratio of the surface layer to phytoplankton to determine the value of full depth since there was no direct data for the deep layer. Also, there is a lack of data on fish density in Pujada Bay, so all of them were directly considered as 0 in the calculation using the NPZF model.

Table 4.5 Detailed location information of observation site

Location	Latitude	Longitude
Observation Site (referred to CMEMS[33])	6°45'N	126°30'E

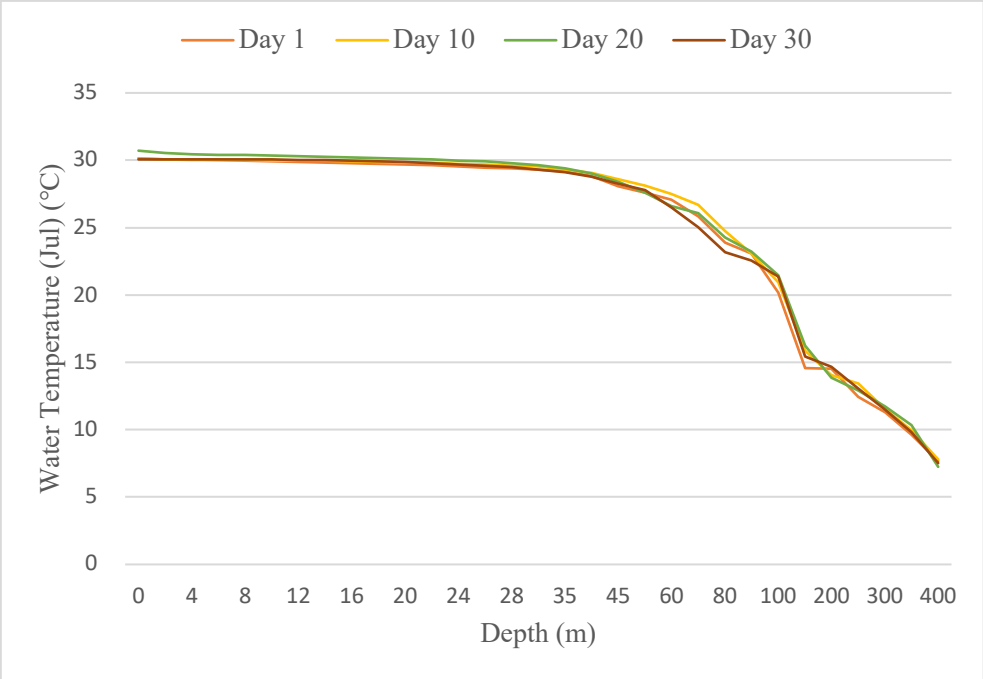

Fig. 4.19 Open boundary data of water temperature (July)

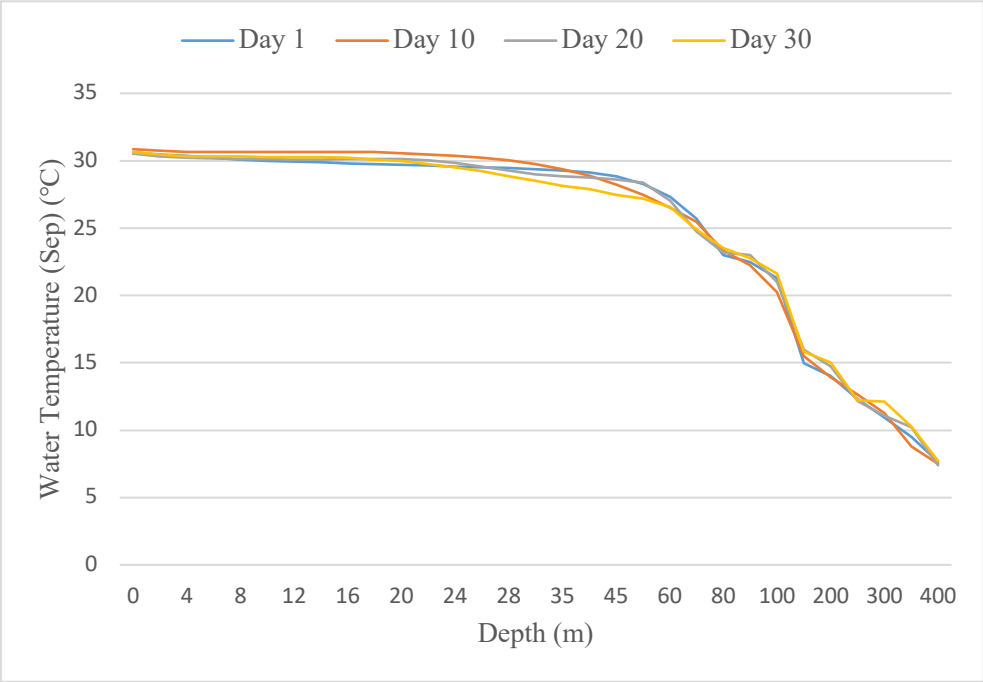

Fig. 4.20 Open boundary data of water temperature (September)

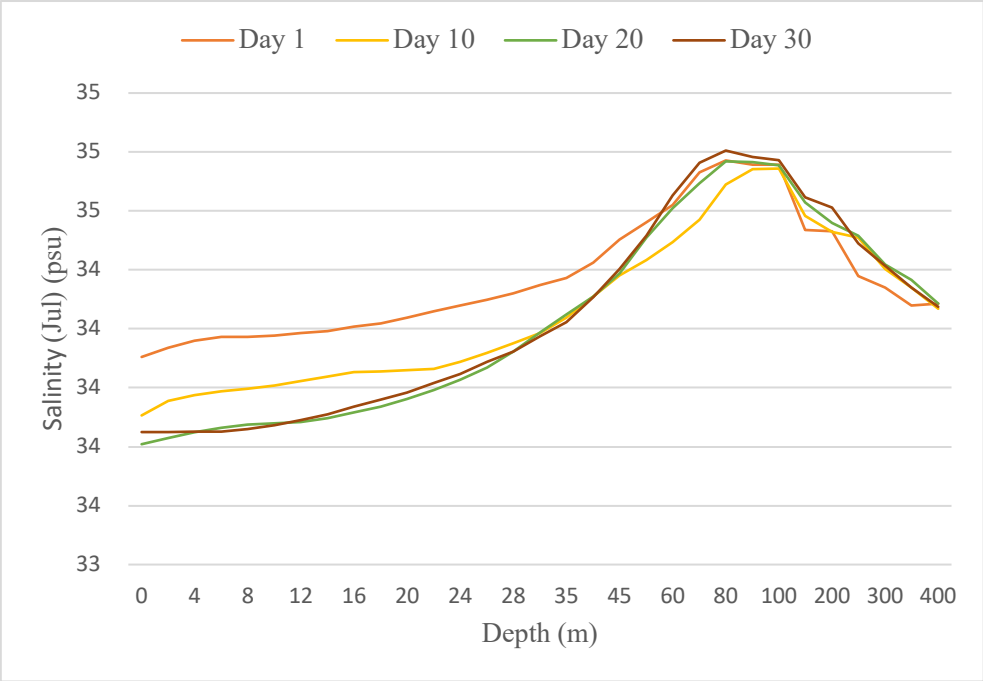

Fig. 4.21 Open boundary data of salinity (July)

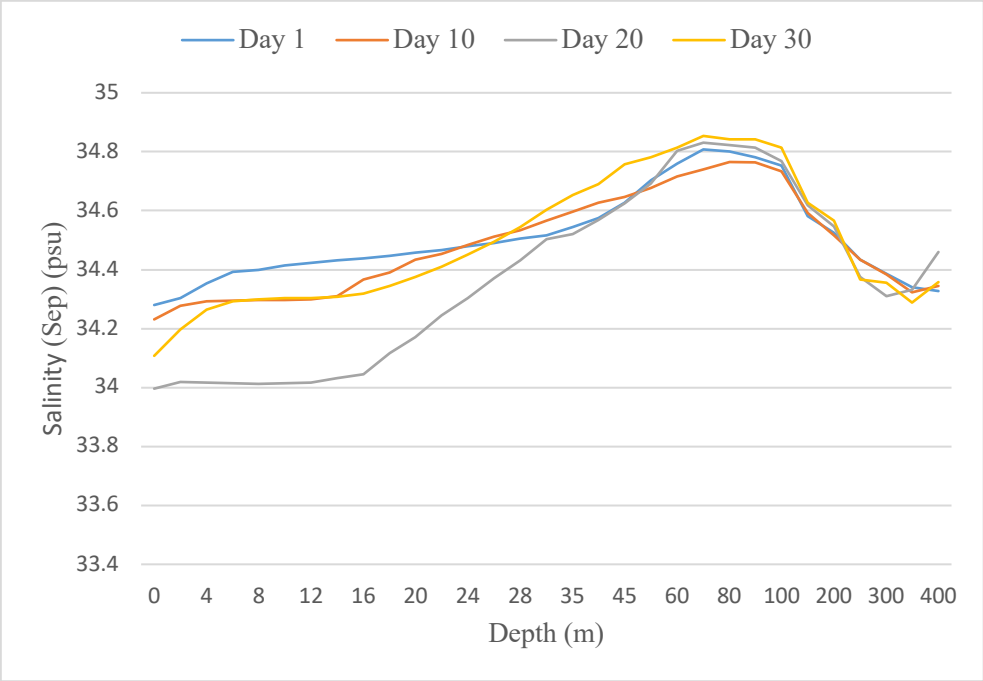

Fig. 4.22 Open boundary data of salinity (September)

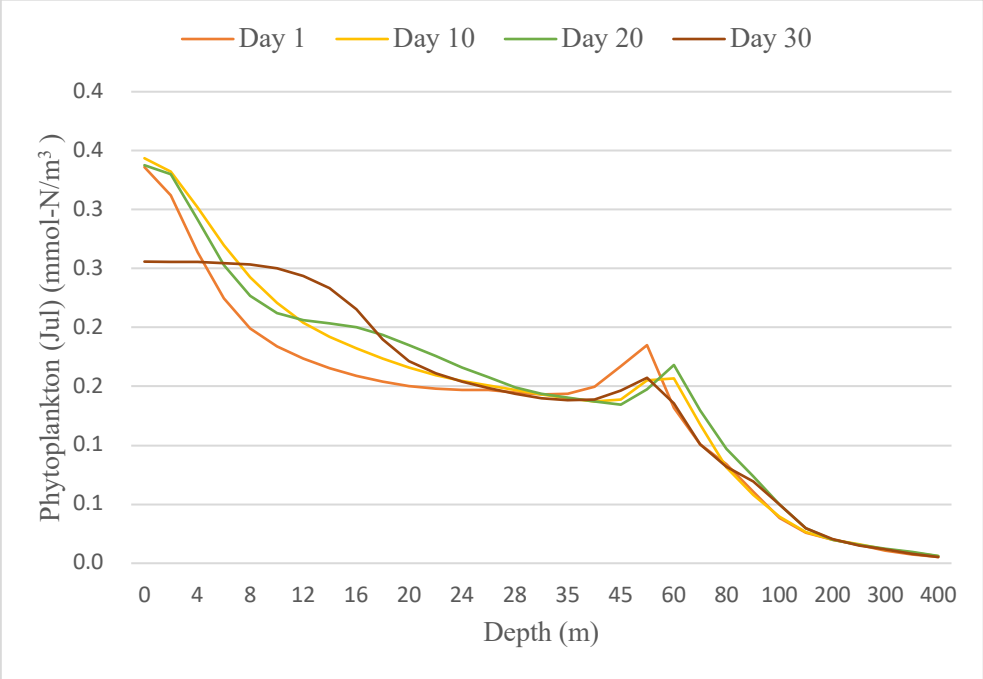

Fig. 4.23 Open boundary data of phytoplankton (July)

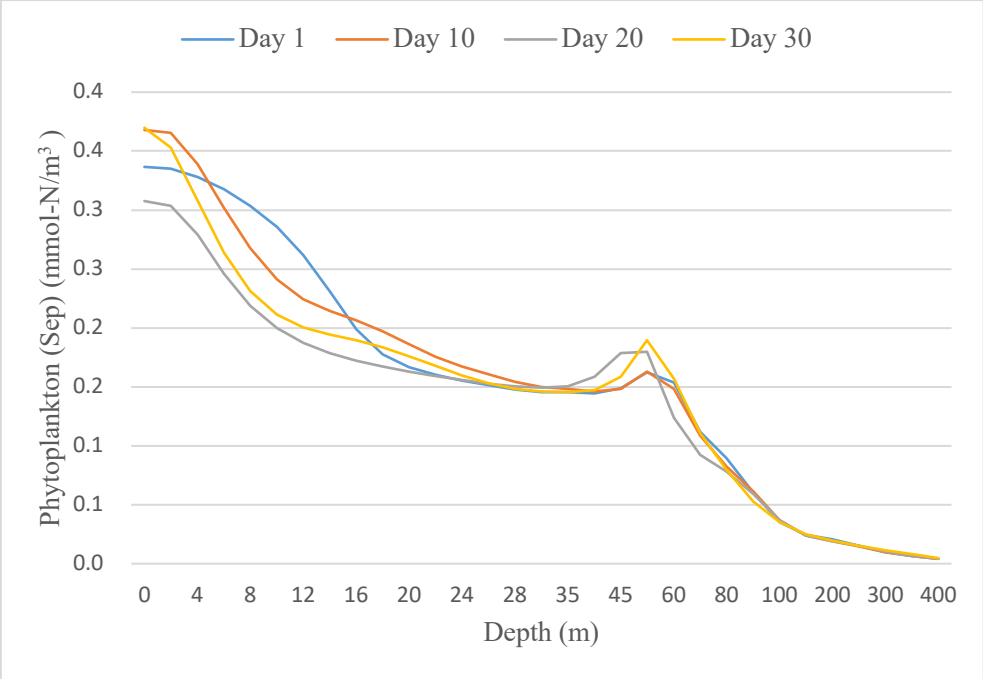

Fig. 4.24 Open boundary data of phytoplankton (September)

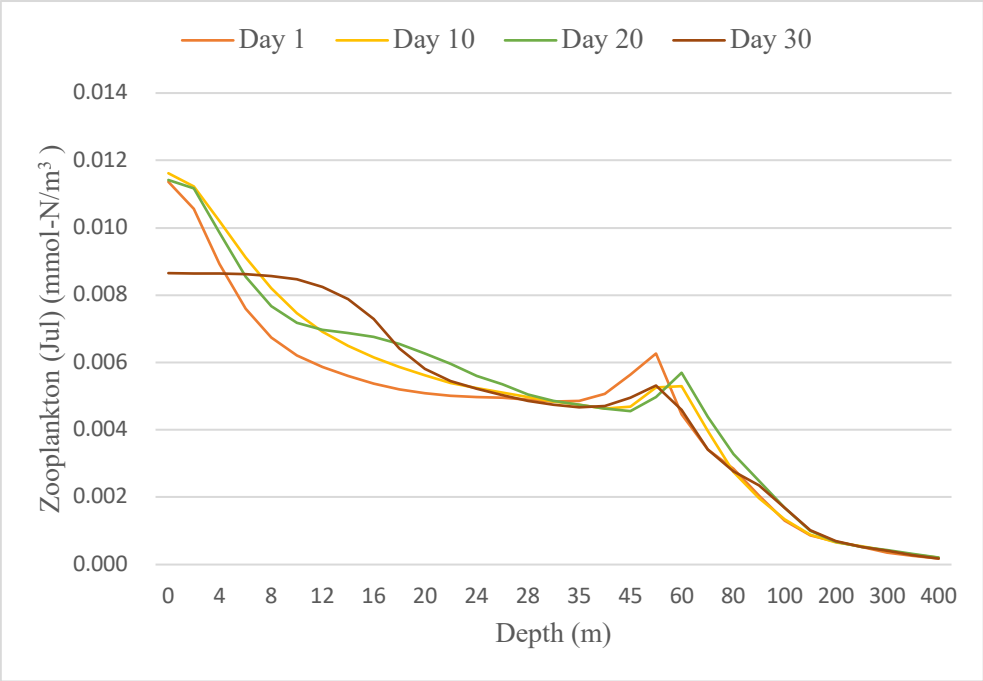

Fig. 4.25 Open boundary data of zooplankton (July)

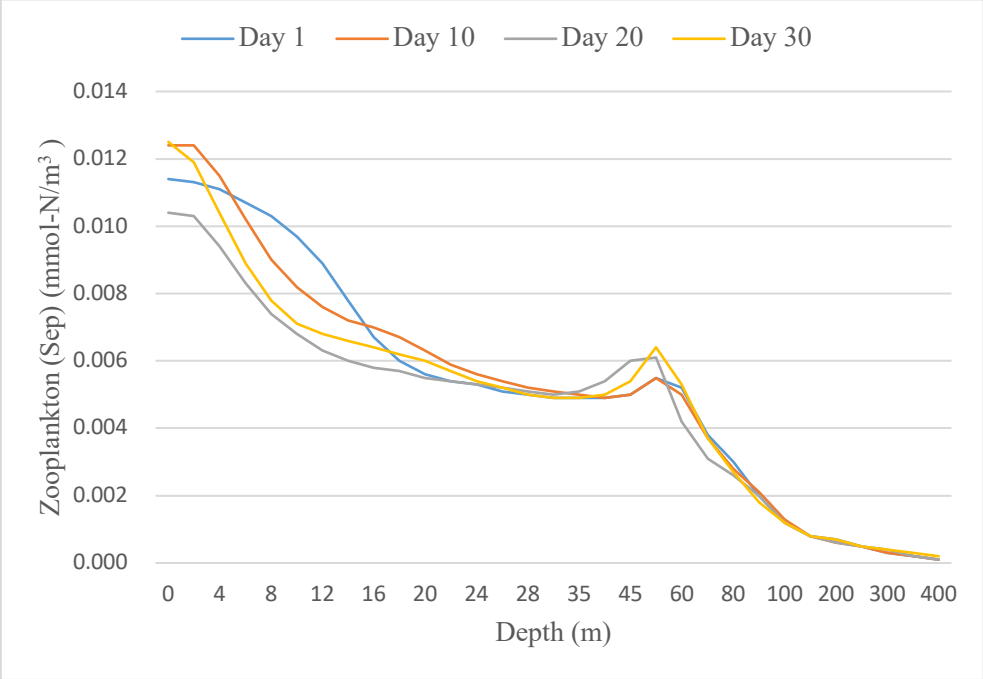

Fig. 4.26 Open boundary data of zooplankton (September)

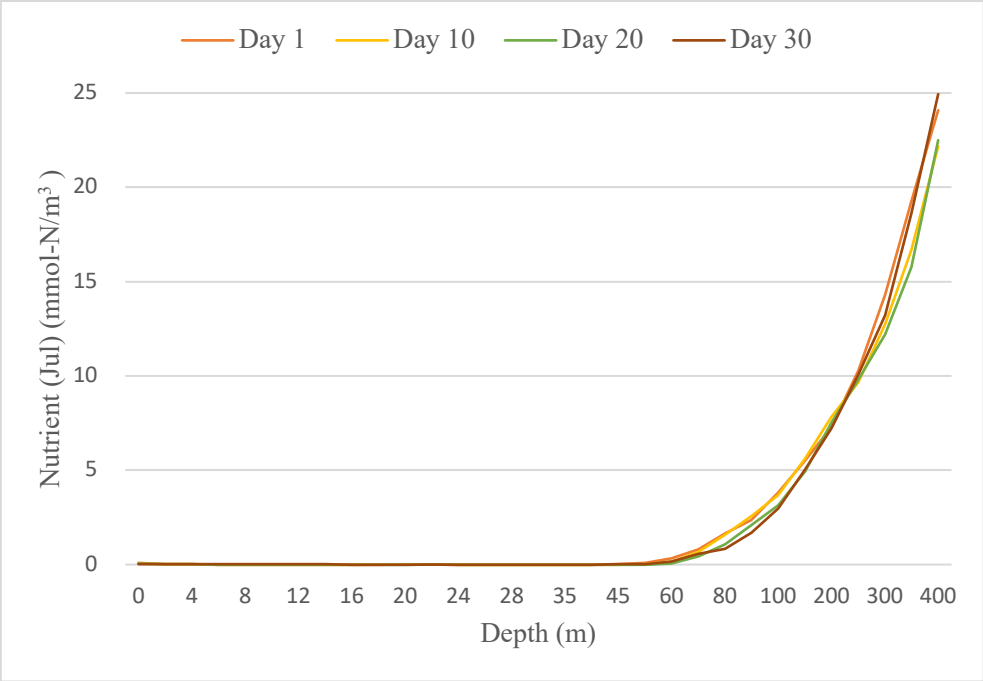

Fig. 4.27 Open boundary data of Nutrient (July)

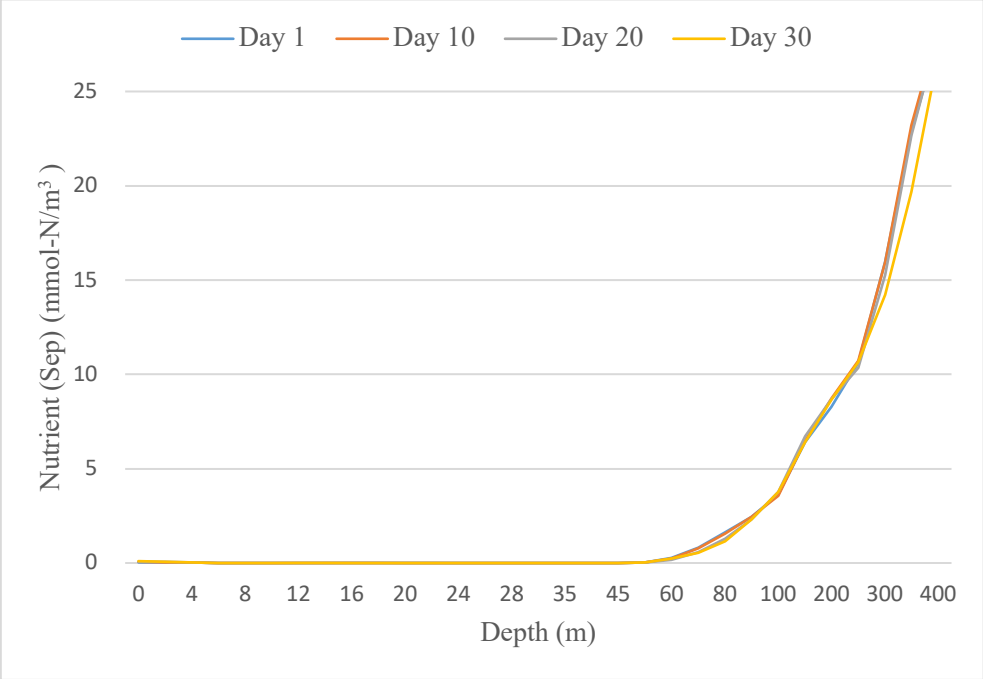

Fig. 4.28 Open boundary data of Nutrient (September)

4.3.4 River data

Data of three rivers were selected to input into MEC-NEST model. They were Magum River, Matiao Creek and Pahamutang Creek. Location information of river mouths are shown in Fig. 4.1 and more detailed information in Table 4.6.

Table 4.6 Information of rivers in Pujada Bay

Location	Magum River			Matiao Creek			Pahamutang Creek		
Longitude	126.24808	i	16	126.22720	i	51	126.23384	i	54
Latitude	6.76997	j	12	6.94309	j	98	6.93824	j	95
Parameter	July	September		July	September		July	September	
Discharge (m^3/s)	0.33	0.11		0.09	0.03		0.09	0.03	
Temperature (℃)	23.74			27.47			28.97		
Salinity (psu)	0.14			0.34			4.69		
Phytoplankton ($mmol\text{-}N/m^3$)	0.3366			0.3366			0.3366		
Zooplankton ($mmol\text{-}N/m^3$)	0.0114			0.0114			0.0114		
Nutrient ($mmol\text{-}N/m^3$)	0.1435			0.1435			0.1435		
Fish density ($mmol\text{-}N/m^3$)	0			0			0		

It should be noted here that the only river ecosystem data that can be collected at present are for September 2020. Considering that the river does not have much flow even during the wet season and its impact on the bay environment is minimal, the river data for July were simply treated as the same values as those for September. And the flux of the river in July was a numerical projection based on the rainfall of both months.

4.3.5 Initial data

The data in this part were mainly from the annual report from the Philippine side, and some missing data were complemented by data from observation sites outside the bay (referred to CMEMS[33]). Note that it was assumed that the environment inside the Pujada Bay is just like that outside the bay and at the beginning of the simulation, the initial data in the grids of the bay are uniformly the same. For the practical simulation, all 31 layers of the grids were assigned with different values, the following Table 4.7 only shows part of the data for the surface (2 m), medium (150 m) and bottom (300 m) layer.

Table 4.7 Initial data at different depths in the bay

Parameter	Unit	July			September		
		Surface	Medium	Bottom	Surface	Medium	Bottom
Temperature	℃	30.1482	28.0490	9.6544	30.6126	28.8203	9.4948
Salinity	psu	34.1044	34.5027	34.2799	34.2799	34.6278	34.3410
Phytoplankton	mmol-N/m^3	0.3360	0.1670	0.0075	0.3366	0.1488	0.0064
Zooplankton	mmol-N/m^3	0.0114	0.0056	0.0003	0.0114	0.0050	0.0002
Nutrient	mmol-N/m^3	0.0821	0.0063	19.2773	0.0469	0.0067	22.8408
Fish density	mmol-N/m^3	0	0	0	0	0	0

4.4 Output Sites for Simulation Results

Since the main objective of this research is on predicting and assessing the possible impacts of future human activities on the bay, two output points were selected for the demonstration of the MEC-NEST model simulation results. They were in the northeastern part of the inner bay, which were close to the largest city along the coast, Mati, and was within the area that most likely to be affected by human activities. See Fig. 4.29 and Table 4.8 for detailed information.

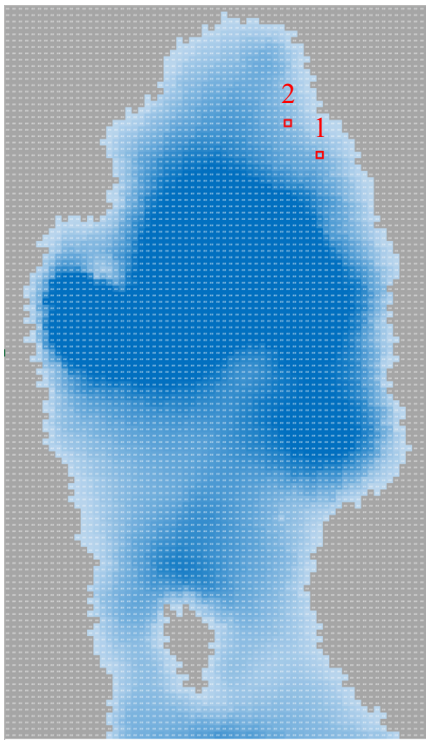

Fig. 4.29 Location of output sites on the map

Table 4.8 Location information of two output sites

Output site	i	j
Site 1	51	91
Site 2	46	96

Chapter 5. Simulation Results and Analysis

5.1 General Overview

In this chapter, the simulation results were compared to the observation data. Usually, this step is expected to testify the accuracy of numerical model. However, in this research, this premise must be mentioned that the observation data used in this chapter are all from one observation site outside the bay (sourced from CMEMS[33]). Detailed location information can be found in Table 4.5. Although in the computational condition it was assumed that the values of the parameters inside Pujada Bay are approximate to those outside the bay, this assumption could not be followed in the validation of the simulation results. Therefore, in this chapter, all observation data were used only for the reference of numerical ranges but not as a basis for judging the accuracy of the model simulation.

In the part of physical simulation, the common practice was conducted on the following components: tidal elevation, current flows, and water temperature as well as salinity. The tidal elevation in this model was mainly affected by that at the open boundary, while current flows, water temperature, and water salinity vary a lot among the bay. Generally, current flows are more readily affected by the external forces like tidal forces or wind frictions. Since only the simplest tidal simulation was used in this research, the fidelity of this part cannot be guaranteed. In the following discussion, this part will be neglected due to practical reasons. The detailed analysis of water temperature and salinity is described in the following sections.

Following the physical analysis, ecosystem analysis plays a pivotal role in evaluating the effects of human activities. However, the observation data of ecosystem environment, unlike the data of physical environment, were hard to be collected. In particular, the distribution of zooplankton data in the vertical direction in this research used a proportional conversion with phytoplankton data (see 4.3.3 for details). This coarse data-processing operation brought a loss in resolution and made it difficult to analyze ecosystem environment as done in physical environment. As a compromise, this research focused on the coarse reduction of the bay overall environment and the plausibility of the simulation, which paved the way for the subsequent scenario setting.

The simulation results on all the parameters were compared at the depth within 5 m during the period of July 1, 2020 – July 30, 2020, and September 1, 2020 – September 30, 2020 (Fig. 5.1 to Fig. 5.6) since the water quality in the surface layer is more influenced by human activities, and also in turn has a profound impact on the coastal population. The horizontal axis and vertical axis of comparison are fixed, and the legend of figures follow the same rules, in which the red crosses represent the observation value and the lines represent the simulation results from output site 1 and site 2 (refer to Fig. 4.29 and Table 4.8).

5.2 Physical Environmental Variation

5.2.1 Water temperature

Simulation results of water temperature at surface in July and September is shown as Fig. 5.1 and Fig. 5.2. Generally, the simulated water temperature successfully reproduced the diurnal fluctuation tendency but remained difference between the time variations. The fluctuation of the simulation results for both months were within reasonable values. The simulation of July deviated from the observation data in the second half of the month and didn't show drastic temperature variations as the actual observation. The simulation results for September showed the same trend as the observation, but with some deviations in the timeline.

Apparently, the variation of water temperature in the bay was partially simulated, but further pursuit is still needed in some details. There are many possible reasons for errors, besides anthropogenic impacts that may induce drastic fluctuations, 1) physical factors, such as wind pressure or sudden short-lived rainfall; 2) ecosystem factors, such as the screening effect of aquatic organisms; 3) simulation approximations, such as the precision of the bulk equation and stratification function, have an unavoidable effect on the simulation gaps.

In summary, there is still room for improvement in simulation accuracy, but these gaps have less impact on the numerical analysis of Pujada Bay in terms of possible future long-time simulations.

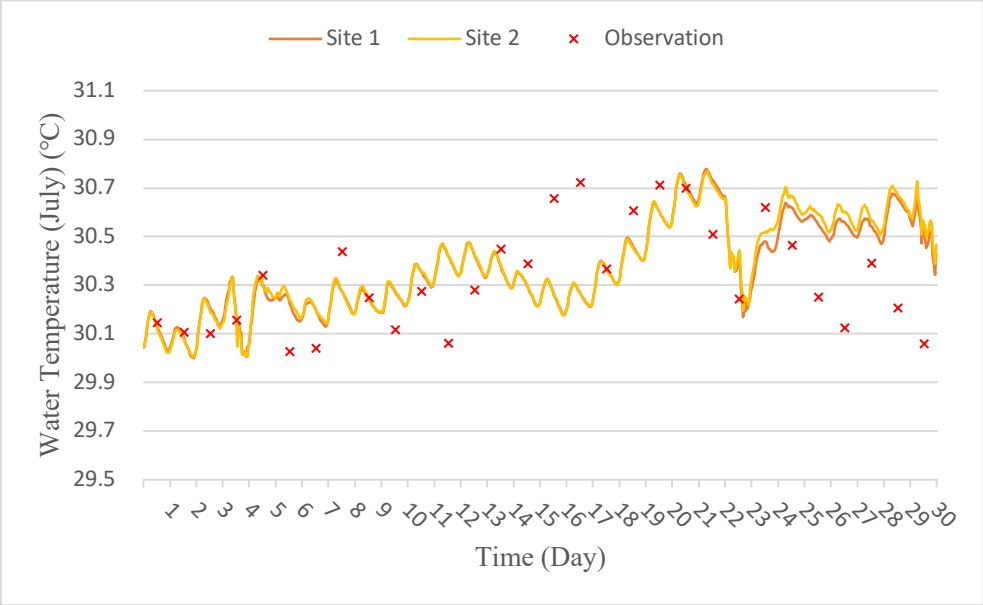

Fig. 5.1 Time series of the water temperature at surface in July

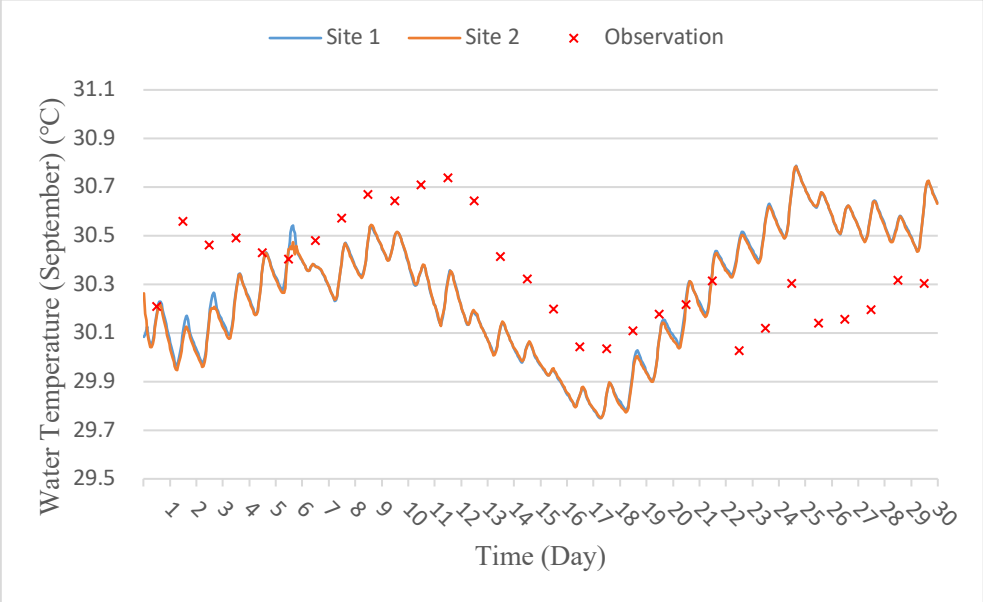

Fig. 5.2 Time series of the water temperature at surface in September

5.2.2 Water salinity

Fig. 5.3 and Fig. 5.4 below show the simulation results for salinity in Pujada Bay. Unlike water temperature, the simulation results showed large differences compared to observation due to the observational difficulty of salinity itself, and this problem was even more pronounced for water surface, where salinity can be affected by a variety of factors.

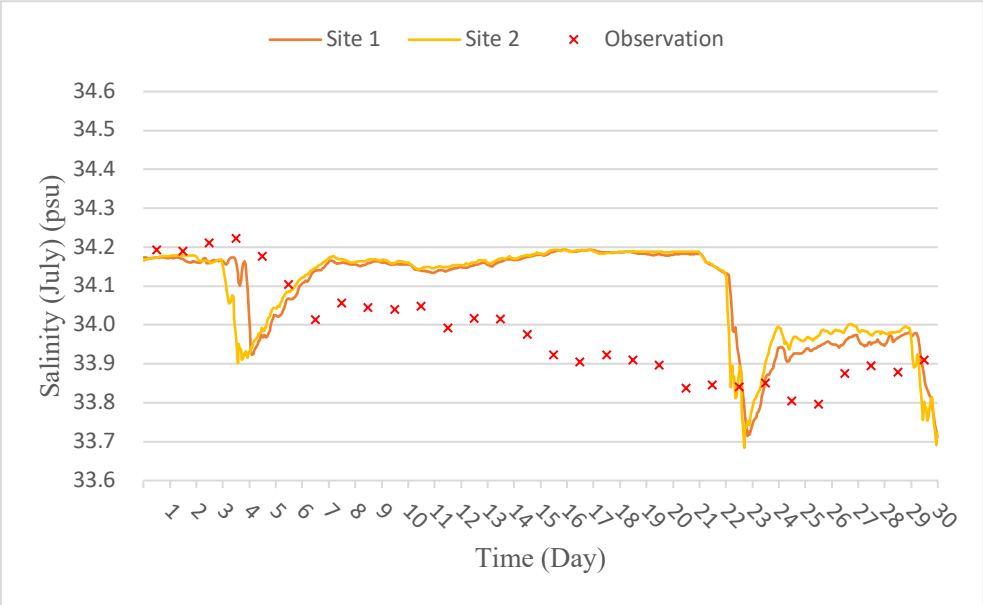

Fig. 5.3 Time series of the salinity at surface in July

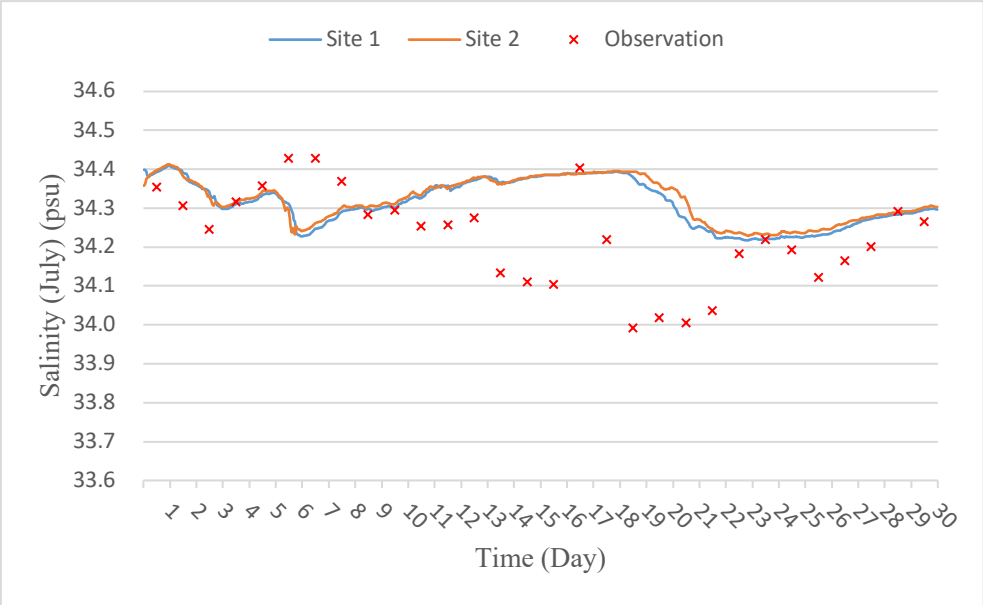

Fig. 5.4 Time series of the salinity at surface in September

Compared to the observation, the simulation of July did not show a linear decreasing trend, but two sudden salinity dips on the fourth day and twenty-third day. After checking with the input data, this phenomenon can be attributed mainly to the precipitation in the climate data (see Fig. 4.11). Since the only input data available were daily precipitation, an assumption had to be made when entering the climate data that the daily precipitation was distributed equally over certain hours. And July is the month with more rainfall, especially on the 4th and 23rd, this idealized assumption was obviously reflected in the salinity of the surface water. The simulation results for September showed a better

trend than July, which can be explained by the less rainfall in September (see Fig. 4.14). In the middle part, the simulation shows a large discrepancy with the observation though the source of error cannot be specified clearly here.

In general, there is a lot of room for improvement in the simulation of salinity. It is difficult to make reasonable adjustments to the simulation results in this research due to the missing input data, but the simulation results have shown the response of the model to environmental changes, so it still has its value in future applications.

5.3 Ecosystem Environmental Variation

5.3.1 Nutrient

Following the comparison of water temperature and salinity, a scrutiny of nutrient levels in the bay is also essential (shown in Fig. 5.5 and Fig. 5.6). However, few conclusions have been made about the nutrient state in Pujada Bay, and the available data are quite scarce, which also hinders this research. Still, this part cannot be taken lightly since the calculation of the competition model was also based on nutrient levels.

The simulation of July showed a good simulation trend, and although the overall values were slightly larger than the observations, they basically fit in their time variation. In the last five days of the simulation, there was a sharp increase in the observation part, and here it is suspected that local anthropogenic activities or tides caused the sudden change in nutrient values. In contrast, the September simulation results did not perfectly reproduce the fluctuations of observational nutrient levels over time. However, the available nutrient observation data themselves have a wide range of variability at different depths of the surface water, which can also be seen to be greatly influenced by various factors, so these errors are considered negligible in this research.

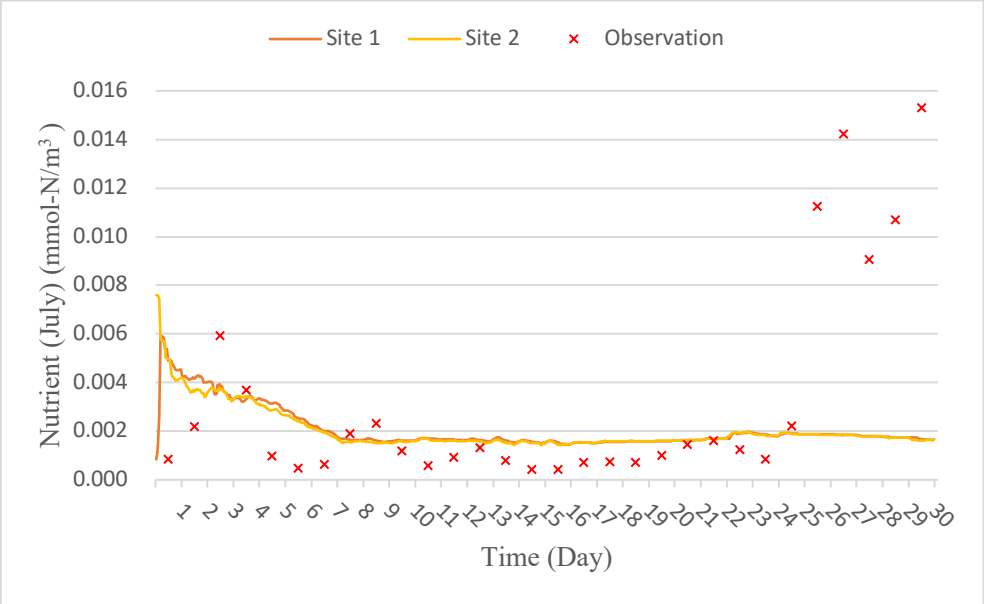

Fig. 5.5 Time series of the nutrient at surface in July

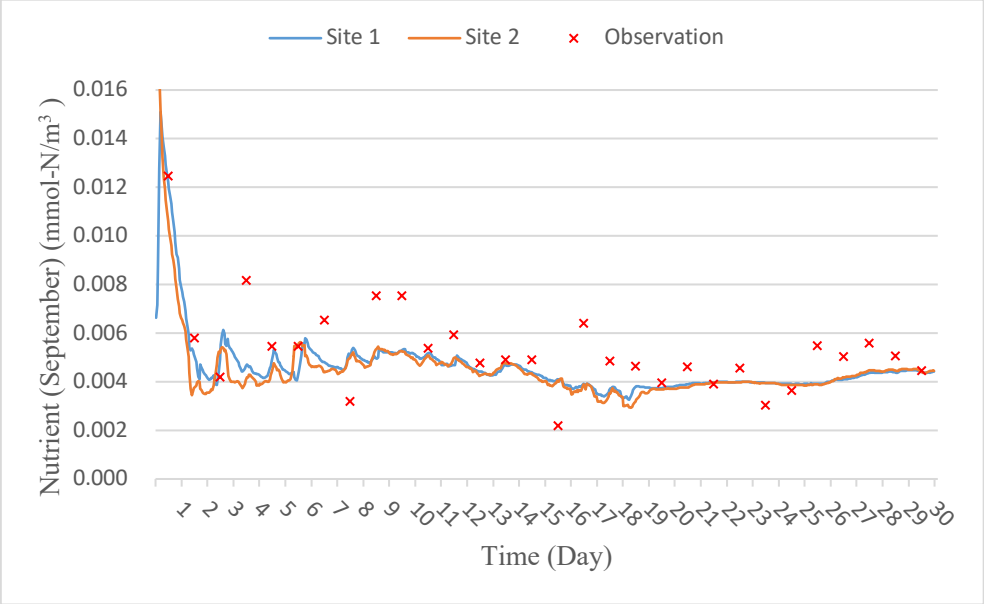

Fig. 5.6 Time series of the nutrient at surface in September

In brief, the simulation of nutrient was relatively successful. Although there were some instabilities at the beginning of the simulation, as the simulation time extended, the simulation became stable and was consistent with the actual observation. And the conclusion that Pujada Bay had a fairly clean water environment at this stage can be drawn at the same time, as its overall nutrient concentrations were quite low.

5.3.2 Phytoplankton

The next parameter simulated by the NPZF model is phytoplankton, and the simulation results are shown in Fig. 5.7 and Fig. 5.8. Usually, concentration of phytoplankton is mainly limited by nutrient concentration and water temperature, while in the model, it is constrained and controlled by multiple transition processes (see details in 2.3.2). Although stable simulations could be performed by adjusting the parameters, the simulation results were still different from the observations.

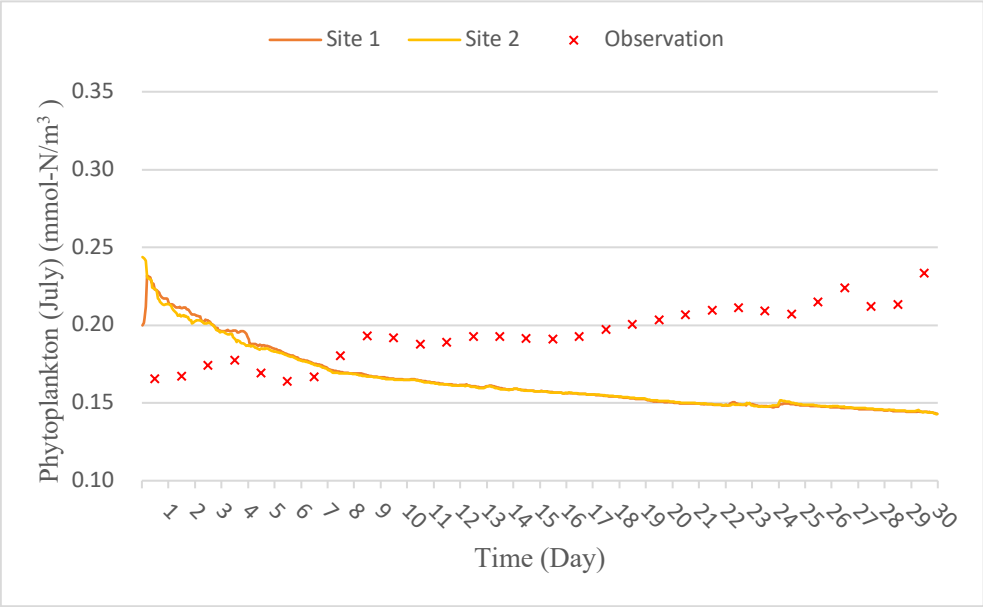

Fig. 5.7 Time series of the phytoplankton at surface in July

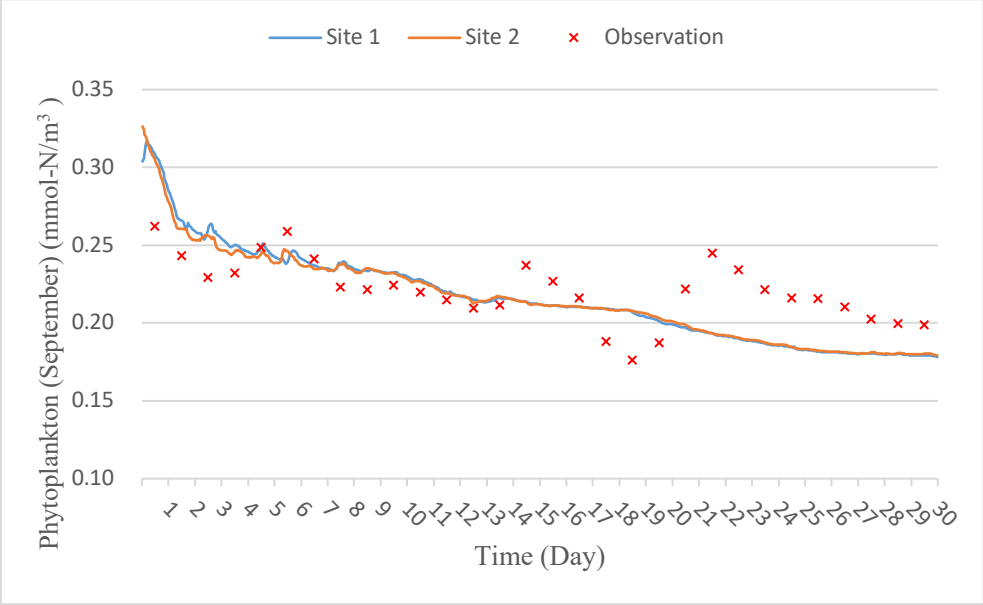

Fig. 5.8 Time series of the phytoplankton at surface in September

In the simulations for both months, although the overall values were within a reasonable range, the trends showed the opposite situation. Excluding the fact that the observation site was located away from the Pujada Bay, the probability that the simulation results in July showed the opposite trend to the observation was that the data related to zooplankton didn't match the real situation. As mentioned at the beginning of this chapter, the input data for zooplankton were simply converted from the phytoplankton data, which can have a large impact on the model calculations. In contrast, the simulation results in September were more consistent with the observation. Although some peaks were not represented in the simulation, the general trend and range of values were close to the observation. The lack of relevant data makes the simulation and follow-up analysis of phytoplankton distribution difficult, and the reliability of the model cannot be confirmed at the present stage, so further studies are still needed.

5.3.3 Zooplankton

The simulation results for zooplankton exhibited a similar situation to those of phytoplankton (shown in Fig. 5.9 and Fig. 5.10). However, zooplankton were less governed by transition processes in the model's calculations (zero effect from fish density) and therefore showed a better trend of variability.

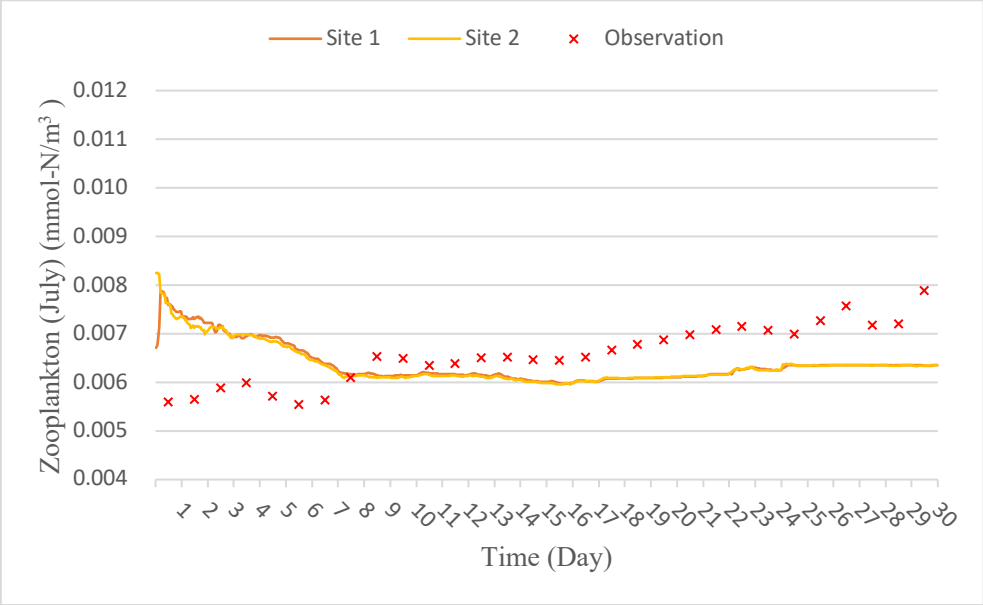

Fig. 5.9 Time series of the zooplankton at surface in July

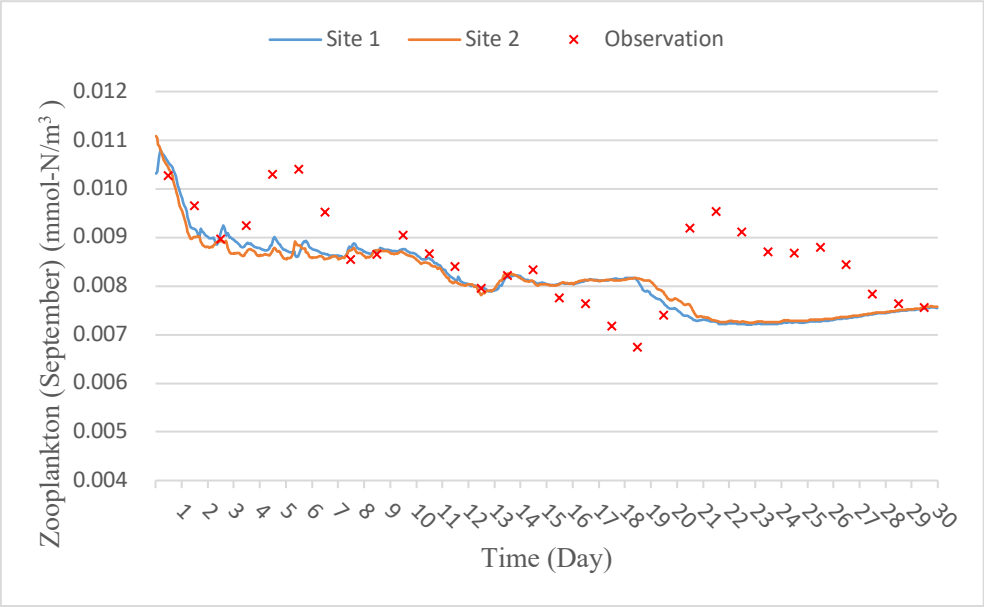

Fig. 5.10 Time series of the zooplankton at surface in September

In the simulation of July, the zooplankton distribution also showed a trend opposite to the observation in the early stages, but it could also be seen to start gradually rebounding in the second half of the month. This proved that the model itself has the ability to simulate and reproduce the real environment, but it was difficult to achieve a more accurate simulation under the existing conditions. On the other hand, the simulation results for September were similar to the phytoplankton part and showed a more reliable accuracy which may thank to the advantage of data fidelity.

5.4 Results of Competition Model

5.4.1 Reproduction and analysis

After simulating the water quality and ecosystem of Pujada Bay using the MEC-NEST model, based on its simulation results, further simulations of the coral-algae competition model were conducted and analyzed in this part. To set the ground for the subsequent scenario setting, the nutrient level and herbivory pressure of Pujada Bay was measured firstly with the current environmental background. It is of concern that in the original calculation of the competition model, these parameters should be derived from experiments or corresponding studies, but this research lacked such conditions, so the final simulation condition was determined by estimating the range here. This certainly makes the

reliability of the model ambiguous but considering the stochastic and probabilistic nature of the model itself, the error in this part doesn't affect the indicative role of the simulation for the bay environment. To make the simulation results clearer and easier, the figures shown here (Fig. 5.11 and Fig. 5.12) are the results of multiple simulations by using simplified simulation conditions.

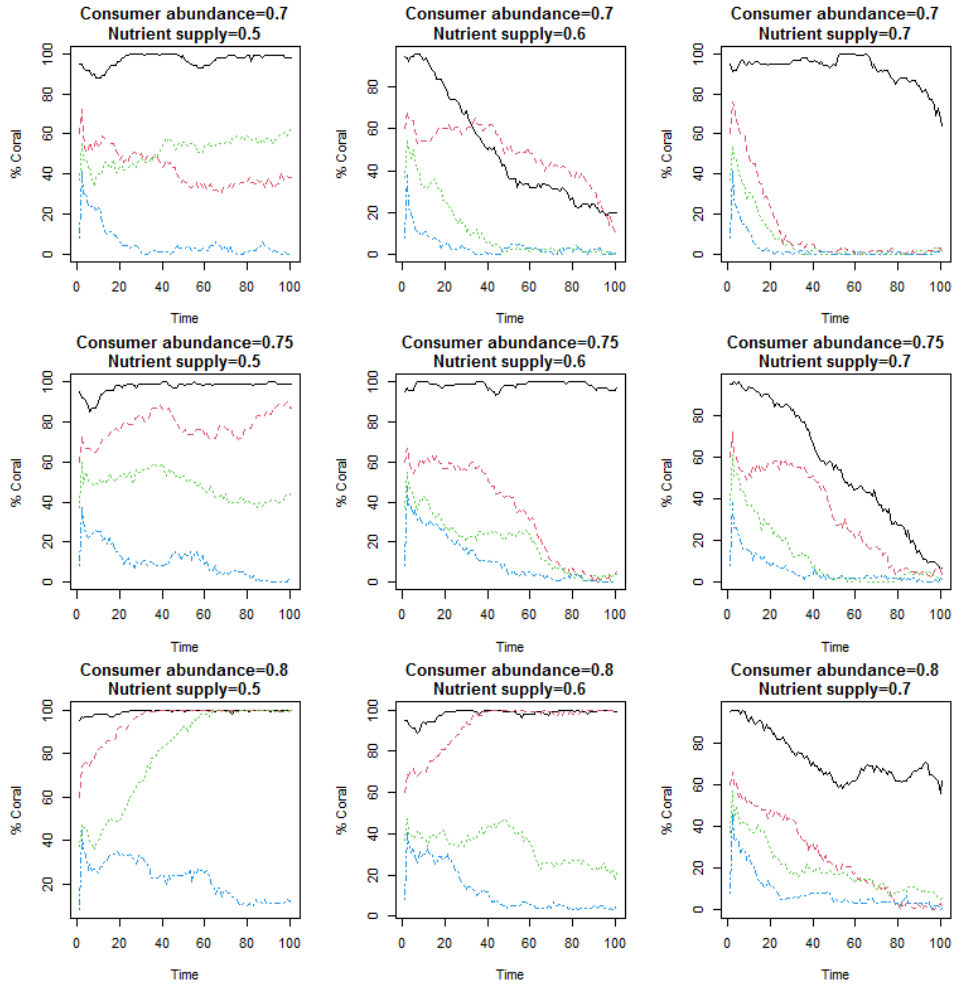

Fig. 5.11 Multiple simulation results of coral abundance

From these figures, the final abundance of corals in the grid where the output sites located was calculated from random initial abundance distributed in a 10% – 90% range after 100 time steps (approximately 3.8 years long) with the interference of different nutrient levels and herbivory pressure. It can be seen that at higher nutrient levels, the abundance of corals decreased significantly. At the same time, it was also limited by herbivory pressure, so the decrease in coral abundance is more moderate in the case of a higher density of local consumer, which is also in line with the perception and facts.

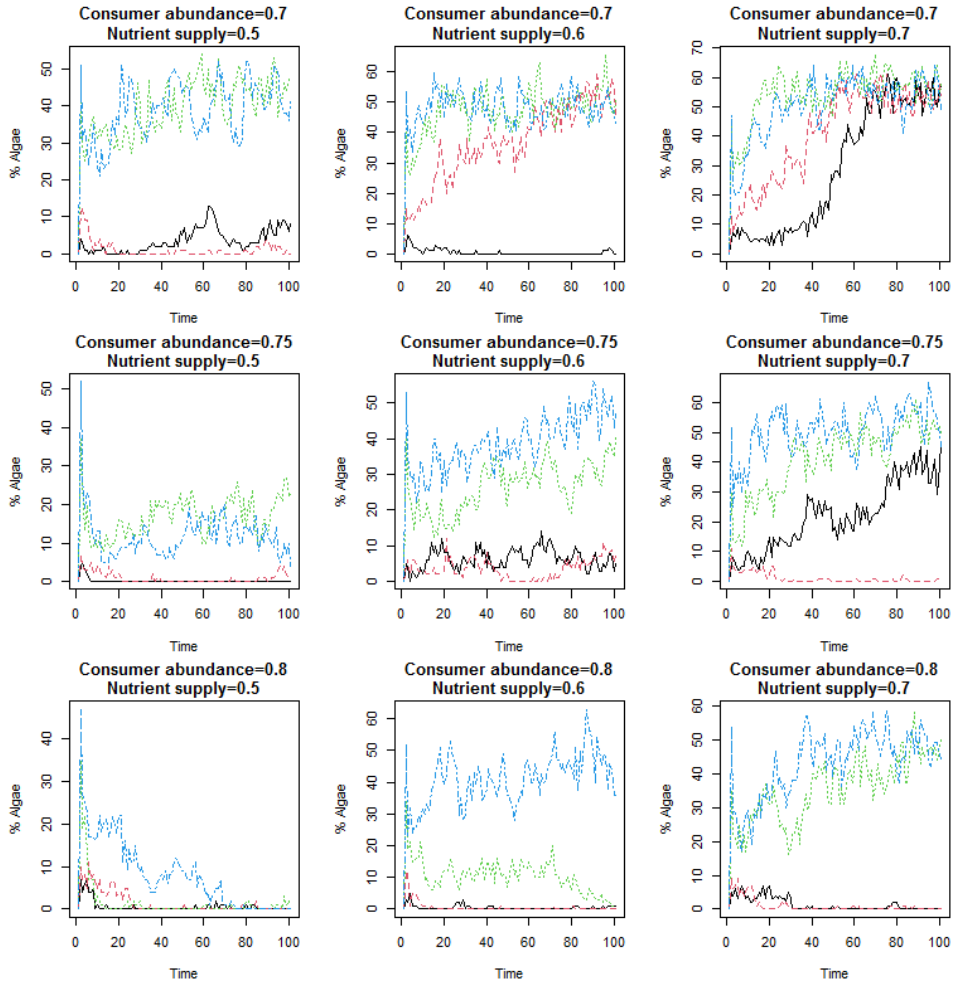

Fig. 5.12 Multiple simulation results of algae abundance

Since algae have two stages that can transform into each other (see 3.2.1 for details), the fluctuations in algal abundance with time step are much more dramatic, but the results still could reflect the exact opposite pattern to coral abundance. With high nutrient supply and low consumer abundance, the algae abundance showed an increasing trend within the simulation grid.

5.4.2 Comparison with field survey data

To further determine the nutrient supply and consumer abundance in Pujada Bay, the simulation results were also compared with the field survey results in this research. The field survey data that are currently available came from a very small area within the bay. The exact location information is shown in Fig. 5.13, while its results are listed in Table 5.1. The sampling location of the field survey

had some distance from the locations of the output sites used in this research, it cannot be simply compared in the real situation, but in the lack of other local data, it was assumed here that the two areas were in a similar situation.

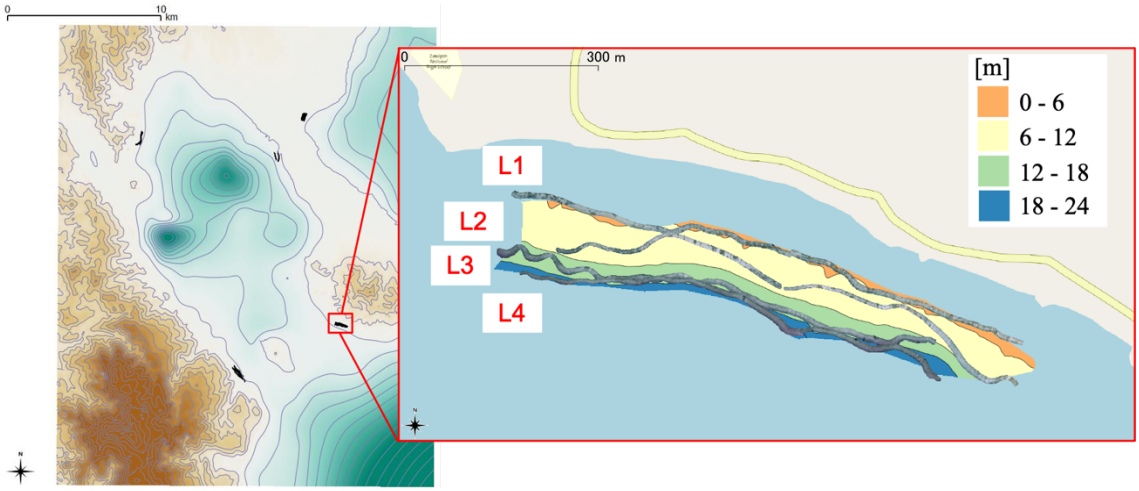

Fig. 5.13Area map for field survey

Table 5.1 Result list of field survey

Line	Coral%	Seagrass%	Sea urchin%	Starfish%	Others%
L1	9.66	10.09	0.29	0.02	79.93
L2	2.23	20.45	0.68	0.02	76.62
L3	0.39	14.40	0.00	0.00	85.21
L4	0.62	8.69	0.02	0.00	90.67
All	3.29	13.07	0.24	0.01	83.39

From the results of the field survey, it was easy to see that the abundance of both coral and algae along Pujada Bay was at a low level. Considering the more stable simulation of coral abundance by the competition model, the coral abundance obtained from the field survey was used as the main basis for the final determination of nutrient supply and consumer abundance. After comparison, it was concluded that the nutrient supply level in Pujada Bay ranged from 0.6 to 0.7, while the consumer abundance ranged from 0.75 to 0.8.

Chapter 6. Scenario Setup and Corresponding Simulation Results

6.1 Nutrient Load from Rivers

Generally, one of the key factors that has a large impact on the environment of a bay is the river that flows into the bay. However, the flow of the rivers along Pujada Bay is very low and the impact on the bay environment is negligible. It can be seen from Fig. 6.1 and Fig. 6.2 that the nutrient concentration of surface layer in Pujada Bay changed less than 0.0003 mmol-N/m^3 (see Table 6.1 for specific value changes). Other input pathways for nutrient loading could have more significant impact on water quality in this bay.

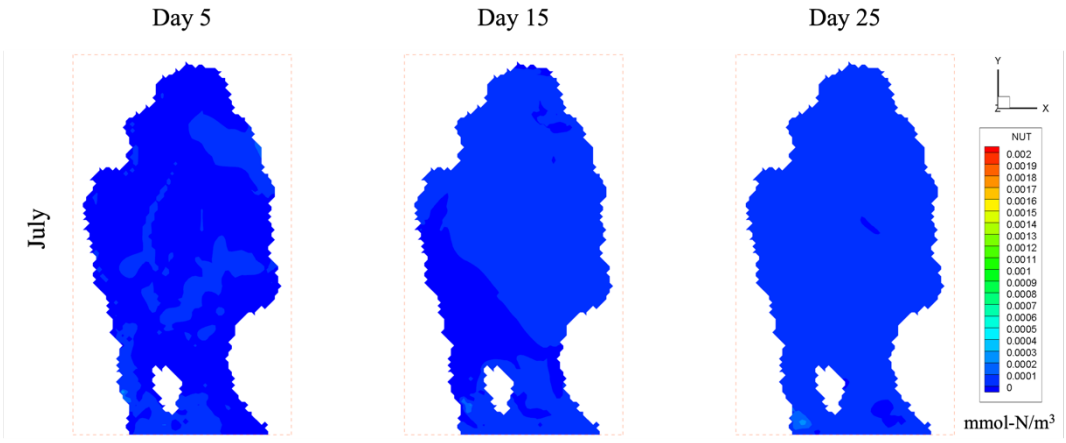

Fig. 6.1 Horizontal distribution of the surface nutrient changes in July (rivers)

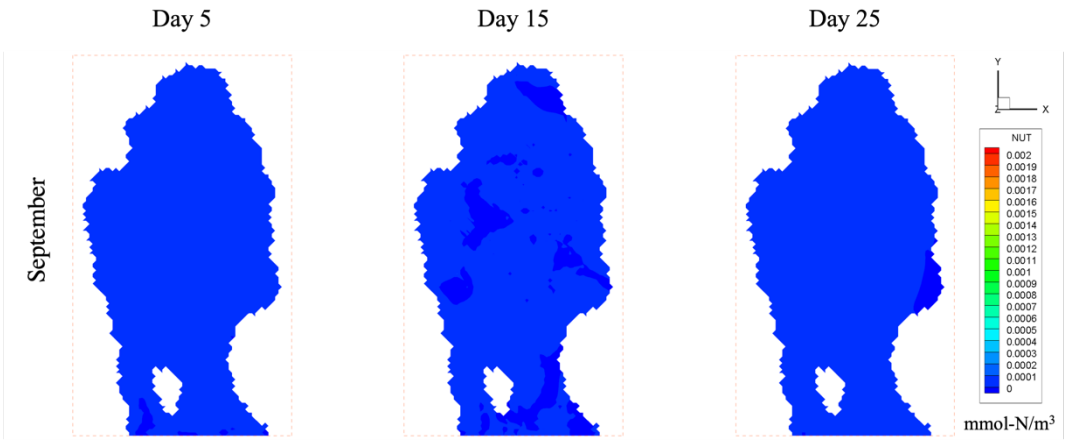

Fig. 6.2 Horizontal distribution of the surface nutrient changes in September (rivers)

Table 6.1 Values used in different scenarios of rivers

River	Magum River (Magum) Matiao Creek (Interco) Pahamutang Creek (Dumping)	
Parameter	July	September
Discharge (m^3/s)	Same as previous	Same as previous
Scene1: Nutrient (mmol-N/m^3)	0.1435 (Initial value)	
Scene2: Nutrient (mmol-N/m^3)	0.4305 (initial value×3)	

6.2 Nutrient Load from Aquaculture Farms

6.2.1 Brief Introduction

Aquaculture uses numerous resources including land, water, feed, fertilizer, energy, capital, labor, and affects ecosystems through the release or extraction of nutrients, the introduction of foreign species, the use of disinfectants and antibiotics, and the alteration of water flows[36]. The amounts and types of waste products resulting from production are usually potential pollutants. On a global scale, the amounts of nutrients released into the marine and brackish water environments were less than the amounts extracted by aquaculture which can be considered as an environmental service provided by aquaculture[37]. But at local scales, high densities of extractive species can still affect ecosystem functioning.

Generally, the nutrient load sourced from aquaculture comes mainly from two forms, fishponds and fish pens/cages. It is cited that 60-80% of nitrogen and phosphorus in feeds enter the culture system as wastes. These may lead to the buildup of organic wastes and dissolved nutrients in the water column, thereby polluting adjacent bodies of water[38]. According to the related research in Manila Bay of Philippines, fish pens/cages had the highest N and P input, which were mainly due to the application of commercial feeds[39]. It constituted 98% of the total annual input of both N and P from feeds, which may be explained by the complete dependence of fish pens/cages on feeds as food for the cultured

species. Here, as similar, the waste from aquaculture, mainly from fish pens/cages, is also considered as one of the possible causes of water quality deterioration in Pujada Bay. Currently, the coastal population of Pujada Bay is still increasing, which will inevitably lead to an increase in the production demand of aquaculture farms, and in turn to an increase in environmental pressure. With the above combined models, this research hoped to make a prediction of the possible future environmental changes in Pujada Bay through scenario construction and corresponding numerical simulations. In this chapter, attention was given to this subject which may cause huge pollution concerns.

6.2.2 Case in Pujada Bay

According to the field survey, there are not too many aquaculture farms along the coast of Pujada Bay at the time of this research, but its impact on the ecosystem of Pujada Bay was already visible. As the satellite photo (Fig. 6.3) shows, in the northwest corner of the bay, there is an area where a concentrated number of fish pens/cages are arranged. This is the only area with relatively large-scale aquaculture farms, which was set as the key simulation target. Some individual small-scale aquaculture farms in other areas were ignored in this research.

Fig. 6.3 Location of the aquaculture farm on the satellite photo from Google Map

6.3 Model Modification and Calculation condition

6.3.1 Model modification

To integrate nutrients discharged from aquaculture farms into the calculation of the NPZF model, an additional nutrient parameter B_{Naq} was added to the original nutrient equation (2.17) in this part. The modified nutrition calculation equation is as follows.

Nutrient (modified) (NUT*)

$$\frac{\partial NUT}{\partial t} = B_6 + B_{11} + B_{201} + (1-\gamma_z)\cdot B_4 + \left(1-\gamma_f\right)\cdot B_{200} + \underline{B_{Naq}} \tag{6.1}$$

Where B_{Naq} represents the nutrient input from aquaculture. This equation was only used in the calculation grid with aquaculture farms located, while in other grids, this parameter was ignored. To facilitate the calculation, parameter B_{Naq} was converted from daily nutrient inputs using the following equation.

Nutrient inputs from aquaculture

$$B_{Naq} = \frac{Naq_D}{24\times 3600} \tag{6.2}$$

Where Naq_D represents the daily nutrient input from aquaculture. Since no field data are available, this process parameter can only be estimated from data of other research. The specific value of Naq_D will be mentioned in the next section.

6.3.2 Calculation condition

Since studies around Pujada Bay are relatively sparse, there are no data related to aquaculture now. However, by comparing and calculating the data with those of similar areas, we can roughly estimate the nutrient emission. As a reference, data related to aquaculture in Manila Bay[39] were used in this research. By comparing the distribution area of the fish cages between the two bays, the specific value of the parameter Naq_D can be estimated from the annual nutrient input from the aquaculture farms in Manila Bay. The value and input location used in this research can be found in Table 6.2.

Table 6.2 Value and location of the modified parameter

Symbol	Parameter		Value		Unit
Naq_D	Daily nutrient inputs from aquaculture		1.2		mmol-N/m^3/day
Location of input grid	i	21	j	98	

Although there is no uniform nor specific value for the setting depth of fish pens/cages, it is simplified here that all nutrients are released into the surface exchange flow. Also, because of the small scale of the aquaculture farms in Pujada Bay, only one 200 m × 200 m grid was set up as the discharge location. Other simulation conditions were consistent with those described in the previous chapter (see Chapter 4 for detail). The location of the output sites, which indicate the key areas to be examined, also remained unchanged from the previous ones (can be found in Table 4.8).

6.4 Corresponding Simulation Results

Since the impact of aquaculture on the bay environment is mainly the nutrient load due to feeds input, this part put the focus on the before and after comparison of simulation results for nutrient concentrations.

6.4.1 Horizontal distribution

The impact of aquaculture pens/cages and the transport of nutrients to the whole Pujada Bay can be further underpinned by the horizontal quality distribution using the simulation results. Fig. 6.4 and Fig. 6.5 show the numerical changes of the before and after values of nutrient concentrations at surface layer in the bay without and with the impact of aquaculture, the gradual diffusion of nutrients in the bay over time can be seen in the figures.

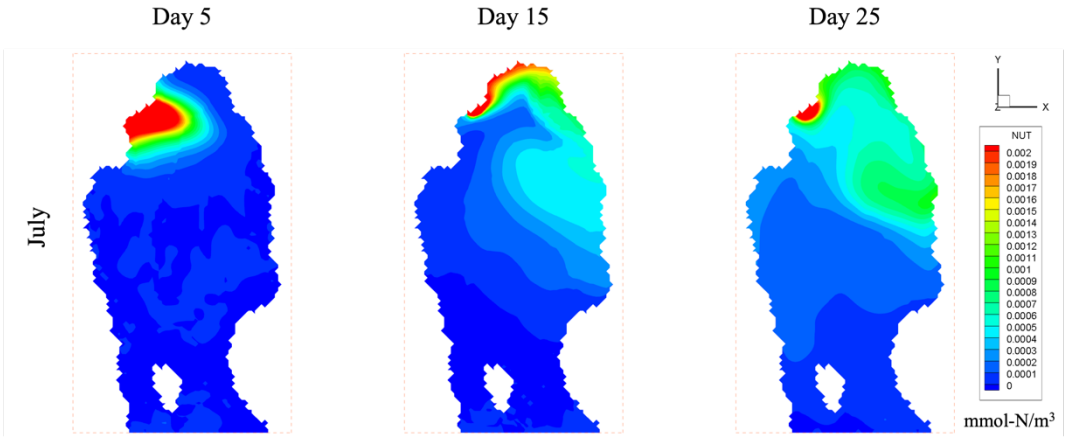

Fig. 6.4 Horizontal distribution of the surface nutrient changes in July (aquaculture)

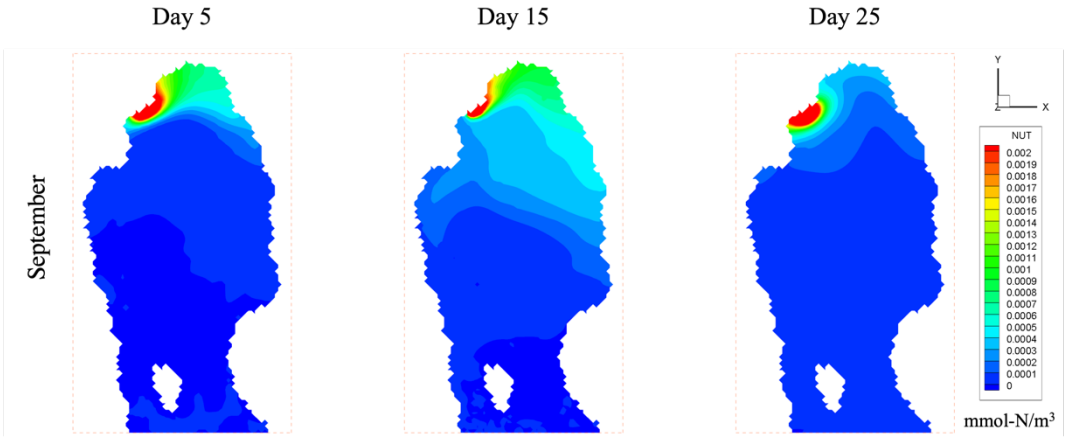

Fig. 6.5 Horizontal distribution of the surface nutrient changes in September (aquaculture)

In general terms, nutrient input mainly affected the area in the northern part of the bay. The south-to-north winds (see Fig. 4.16 and Fig. 4.18 for detail) may be a cause of nutrient accumulation in the northern part of the bay. The nutrients will spread relatively further in July due to the current movement. Meanwhile, water quality was more affected in September, which may be because the initial condition of September itself had a relatively higher nutrient level than July, and with less rainfall, the nutrient concentration on the surface is less diluted.

6.4.2 Nutrient variation under the impact of aquaculture

With an understanding of the overall nutrient distribution in Pujada Bay, it was confirmed that the two output sites set in the model would be affected by aquaculture activities. Then, the nutrient variation

of the simulation results from these two output sites was verified. Since the final aim of this chapter is to compare the variation of coral and algae abundance with increased nutrient supply, here we checked the simulation results of the output sites, considering the depth of coral distribution. To facilitate the final calculation, the variation of nutrient concentration with simulation time was ignored here, and a direct calculation of the average value was taken instead. The corresponding results are shown in Table 6.3.

Table 6.3 Average nutrient for Sites 1 and 2 with and without the impact of aquaculture

NO.	Site 1		Site 2	
Whether affected by aquaculture	No	Yes	No	Yes
Average nutrient of Jul (mmol-N/m^3)	0.0022	0.0030	0.0020	0.0029
Average nutrient of Sep (mmol-N/m^3)	0.0048	0.0053	0.0045	0.0051

After further calculations, it was concluded that the nutrient level under the impact of aquaculture was basically 1.22 times higher than when it was not affected. This conclusion would be used in the calculation of the competition model.

6.4.3 Variation in coral abundance and algae abundance

Returning to the coral-algal competition model, since the conversion of local and global nutrient supply is simply linear in this model (as explained in 3.2.2), the multiplicity of nutrient supply enhancement can accordingly be regarded as equal to the multiplicity of nutrient concentration enhancement. It was already known that the range of nutrient supply in Pujada Bay without considering aquaculture was 06 to 0.7, and on top of that a new nutrient supply level could be substituted into the calculation. The new simulation results obtained are shown in Fig. 6.6 and Fig. 6.7.

Compared to Fig. 5.11, cases that coral abundance reduced was increased under higher nutrient supply conditions, which was also consistent with prediction. In most cases, coral abundance eventually moved to an extremely low level, which also implied a high probability that coral abundance would be replaced by other benthic communities under conditions of high nutrient supply. The algae

abundance, on the other hand, did not show a very significant change. This might be because the algae abundance is limited more by the consumer abundance, and the rise in algae abundance could be observed in the case of low herbivory pressure (the first case in Fig. 6.7). In any case, it is feasible to reflect the ecosystem response to environmental changes in Pujada Bay through this competition model.

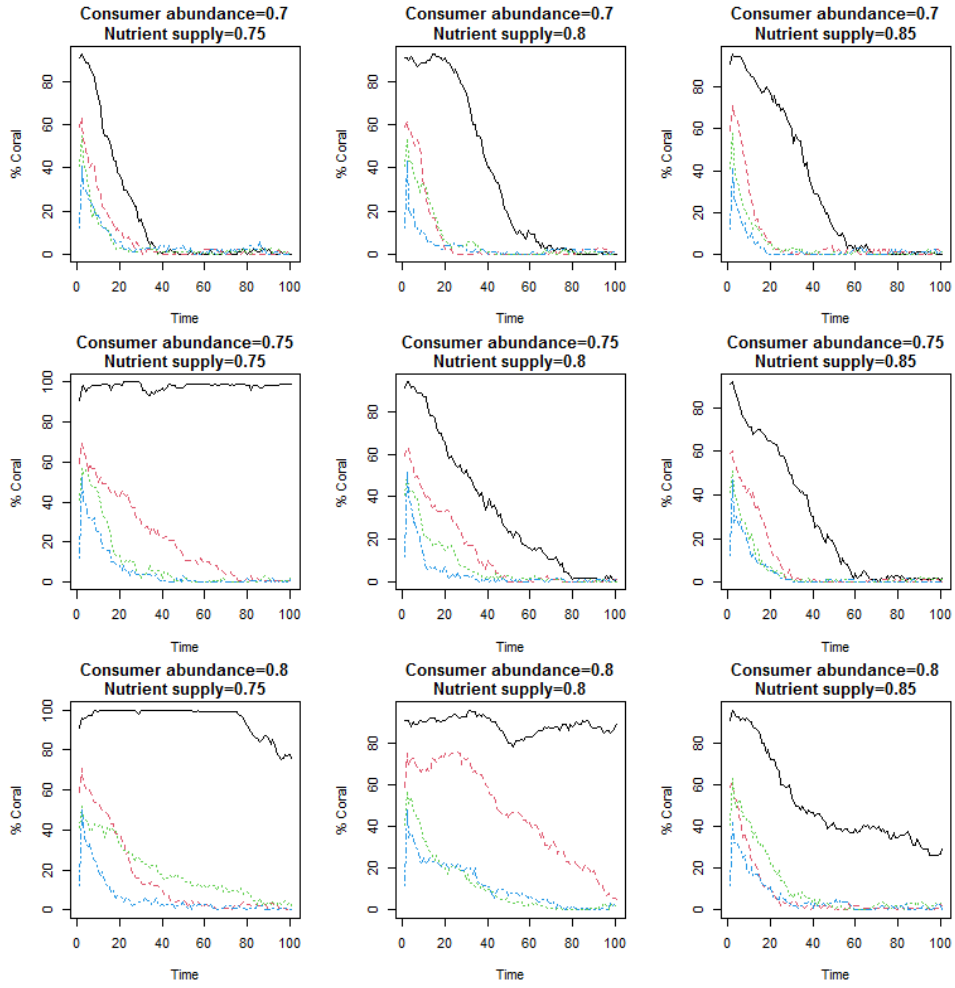

Fig. 6.6 Multiple simulation results of coral abundance under the impact of aquaculture

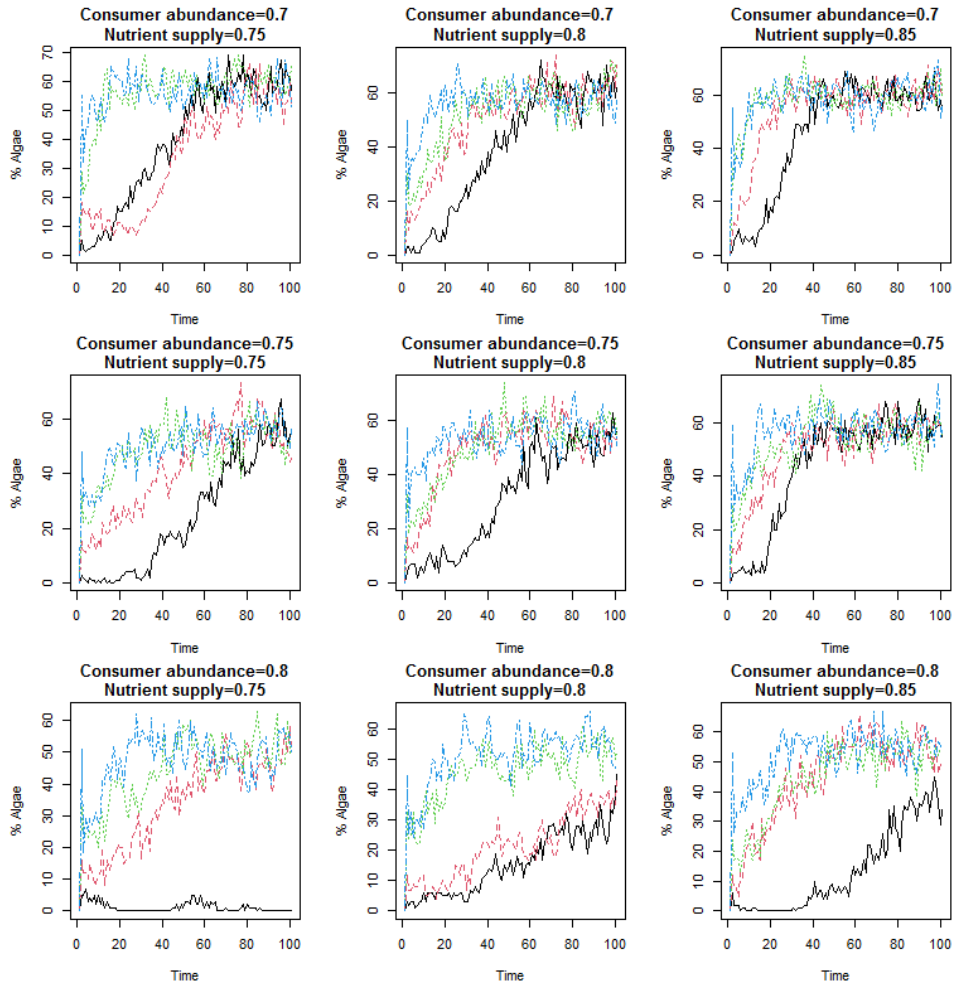

Fig. 6.7 Multiple simulation results of algae abundance under impact of aquaculture

Chapter 7. Comprehensive Analysis and Discussion

7.1 Conclusions

In this research, MEC-NEST Model has been expanded by introducing the coral-algae competition model and applied to the Pujada Bay to understand the current water quality and ecosystem environment, then further to elucidate the possible effects of aquaculture scale expansion on ecosystem. The combined model was stably run, with quantitative reproduction of physical and ecosystem environment. Although the fidelity of the model was not credibly confirmed due to practical reasons, the overall simulation results were still within an acceptable and reasonable range and showed a similar trend to the real situation. Variations in local coral and algal abundance simulated by the competition model also, to some extent, showed the ecosystem response of the bay to environmental changes. The following are the highlights of conclusions:

- The physical environment of water temperature and salinity in Pujada Bay can be reproduced consistently and realistically by MEC-NEST model. The reliability of the simulation can be guaranteed with the availability of complete and reliable input data.
- In the simulation of ecosystem environment, even the simpler NPZF model presented some uncertainty in its simulation results. The ambiguity of this part mainly came from the multiple assumptions that had to be made due to the lack of field data. This requires follow-up data supplementation and recalculations to reassess the accuracy of the model used in this research.
- In this research, two separate time periods of months (July and September 2020) were simulated to analyze the different conditions of Pujada Bay during the wet season and dry season. In terms of results, there was no significant difference between the two seasons, probably because the flows of the three streams flowing into Pujada Bay are very small and not enough to have a significant impact on the overall environment.
- The simulation of the coral-algal competition model, which was introduced to MEC-NEST model for the first time in this research, reflected the pattern of coral and algal abundance variation in response to feedback from both nutrient supply and consumer abundance. Although this model

cannot be used to fully reproduce the real local distribution, it is able to make predictions about possible future environmental changes.

After the first section of this research was completed, scenarios associated with aquaculture were set up to further demonstrate the model's ability to respond reasonably well to possible environmental changes. After model modification and re-simulation, the validity of the model was partially proved. Conclusions as follows could be drawn:

- The nutrient loads inputted by aquaculture could have a large impact on the ecosystem. Although the input of feeds for aquaculture is seasonal and discontinuous, which were not explored in this research, the conclusion that the combined model can reflect the impact of aquaculture won't be compromised.
- The nutrient level in the surface layer of water was elevated under the impact of aquaculture, which indicated that aquaculture might be highly potential as an environmental risk factor for Pujada Bay. The expansion of aquaculture must be limited and scheduled in the background of increasing coastal population.
- The simulation cases that showed reduction in coral abundance under conditions of high nutrient supply also proved that the impact of aquaculture on the ecosystem of Pujada Bay might become critical in the future.

7.2 Future Work

For practical reasons, the biggest drawback of this research was that complete field survey data could not be collected, and thus assumptions had to be used in many processes. Although many previous research has been able to prove the reliability of the MEC-NEST model, whether it can be perfectly applied to Pujada Bay still needs more factual support. Collecting relevant observation data, inputting them into the model and calculating simulations, and then comparing them with the observation to further minimize the errors is a necessary task in the future. A simulation of at least one-year-long simulation period is also more in line with the current need to reproduce the Pujada Bay environment when the required data are available. In addition, more details need to be discussed on the linkage

between the MEC-NEST model and the competition model. This may require certain experimental settings and considering the guiding role of the competition model for environmental protection, this work is thought to be worthwhile.

Reference

[1] Venayagamoorthy, S.K., Ku, H., Fringer, O.B., Chiu, A., Naylor, R.L., Koseff, J.R. (2011) Numerical modeling of aquaculture dissolved waste transport in a coastal embayment. Environ. Fluid Mech. 11, 329-352.

[2] Blumberg, A.F., Mellor, G.L. (1987) A Description of a Three-Dimensional Coastal Ocean Circulation Model. Three-Dimensional Coastal Ocean Models, pp. 1-16.

[3] Haidvogel, D.B., Arango, H., Budgell, W.P., Cornuelle, B.D., Curchitser, E., DiLorenzo, E., Fennel, K., Geyer, W.R., Hermann, A.J., Lanerolle, L. (2008) Ocean forecasting in terrain-following coordinates: Formulation and skill assessment of the Regional Ocean Modeling System. J. Comput. Phys. 227, 3595-3624.

[4] Fringer, O.B., Gerritsen, M., Street, R.L. (2006) An unstructured-grid, finite-volume, nonhydrostatic, parallel coastal ocean simulator. Ocean Modelling. 14, 139-173.

[5] Oschlies, A. (2001) Model-derived estimates of new production: New results point towards lower values. Deep Sea Research Part II: Topical Studies in Oceanography. 48, 2173-2197.

[6] Quere, C.L., Harrison, S.P., Colin Prentice, I., Buitenhuis, E.T., Aumont, O., Bopp, L., Claustre, H., Cotrim Da Cunha, L., Geider, R., Giraud, X., Klaas, C., Kohfeld, K.E., Legendre, L., Manizza, M., Platt, T., Rivkin, R.B., Sathyendranath, S., Uitz, J., Watson, A.J., Wolf-Gladrow, D. (2005) Ecosystem dynamics based on plankton functional types for global ocean biogeochemistry models. Glob. Change Biol. 11, 2016-2040.

[7] Komatsu, K., Matsukawa, Y., Nakata, K., Ichikawa, T., Sasaki, K. (2007) Effects of advective processes on planktonic distributions in the Kuroshio region using a 3-D lower trophic model and a data assimilative OGCM. Ecol. Model. 202, 105-119.

[8] Sandin, S.A., McNamara, D.E. (2011) Spatial dynamics of benthic competition on coral reefs. Oecologia. 168, 1079-1090.

[9] Żychaluk, K., Bruno, J.F., Clancy, D., McClanahan, T.R., Spencer, M. (2012) Data-driven models for regional coral-reef dynamics. ECOLOGY LETTERS. 15, 151-158.

[10] MEC (2000) The Society of Naval Architects of Japan: MEC model workshop. Vol.1, Nov. 2000.

[11] 中田 喜三郎 (Nakata, K.), 田口 弘一 (Taguchi, H.) (1981) 生態-流体力学モテルを用いた内湾の富栄養化過程に関する数値実験内湾の二層潮流モテル. 公害資源研究所彙報. 11, 61-75.

[12] 多部田 茂 (Tabeta, S.) (1994) 多層モテルによる湾内の海水流動に関する数値計算. 博士論文. 東京大学.

[13] Kitazawa, D. (2001) Numerical analysis of the impacts on marine ecosystem by a very large floating structure (in Japanese), Doctoral dissertation. The University of Tokyo.

[14] Zhang, J. (2014) Numerical analysis of integrated multi-trophic aquaculture for biomitigation of marine ecosystem. Doctoral dissertation. The University of Tokyo.

[15] Hakuta, K., Tabeta, S. (2013) Behavioral modeling of Pagrus major in the East Seto Inland Sea. J. Mar. Sci. Technol. 18, 535-546.

[16] Kitazawa, D., Yang, J. (2012) Numerical analysis of water circulation and thermohaline structures in the Caspian Sea. J. Mar. Sci. Technol. 17, 168-180.

[17] Sato, T., Tonoki, K., Yoshikawa, T., Tsuchiya, Y. (2006) Numerical and hydraulic simulations of the effect of Density Current Generator in a semi-enclosed tidal bay. Coast. Eng. 53, 49-64.

[18] Zhang, J., Kitazawa, D., Taya, S., Mizukami, Y. (2017) Impact assessment of marine current turbines on fish behavior using an experimental approach based on the similarity law. J. Mar. Sci. Technol. 22, 219-230.

[19] Mori, C., Sato, T., Kano, Y., Aleynik, D. (2013) Numerical prediction of the diffusion of CO2 seeping from seabed in Ardmuchnish Bay. Energy Procedia. 37, 3503-3506.

[20] Lee, H.-S., Lee, B.-H., sung Kim, K., Kim, S.Y., Park, J.-C. (2019) Tidal current simulation around the Straits of Korea and its application to a speed trial. Int. J. Nav. Arch. Ocean. 11, 474-481.

[21] Xia, Y., Tabeta, S., Komatsuda, S., Duan, F. (2016) The impacts of fishing and nutrient influx from Yangtze River on the ecosystem in East China Sea. Modeling Earth Systems and Environment. 2, 163.

[22] Schroder, A., Persson, L. & De Roos, A.M. (2005) Direct experimental evidence for alternative stable states: a review. Oikos, 110, 3–19.

[23] Dakos, V., Carpenter, S.R., van Nes, E.H. & Scheffer, M. (2014) Resilience indicators: prospects and limitations for early warnings of regime shifts. Philosophical Transactions of the Royal Society of London. Series B: Biological Sciences, 370, 20130263.

[24] Scheffer, M., Carpenter, S.R., Lenton, T.M., Bascompte, J., Brock, W., Dakos, V., van de Koppel, J., van de Leemput, I.A., Levin, S.A., van Nes, E.H., Pascual, M. & Vandermeer, J. (2012) Anticipating critical transitions. Science, 338, 344–348.

[25] Dudgeon, S.R., Aronson, R.B., Bruno, J.F. & Precht, W.F. (2010) Phase shifts and stable states on coral reefs. Marine Ecology Progress Series, 413, 201–216.

[26] Muthukrishnan, R., O. Lloyd-Smith. J. & Fong, P. (2016) Mechanisms of resilience: empirically quantified positive feedbacks produce alternate stable states dynamics in a model of a tropical reef. Journal of Ecology, 104, 1662-1672.

[27] Muthukrishnan, R. & Fong, P. (2014) Multiple anthropogenic stressors exert complex, interactive effects on a coral reef community. Coral Reefs, 33, 911–921.

[28] Muthukrishnan, R. (2013) An Integrated Empirical and Modeling Approach to Evaluate Determinants of Community Structure and Alternate Stable States Dynamics on Tropical Reefs. University of California, Los Angeles, CA, USA.

[29] Randall, J.E. (1967) Food habits of reef fishes of the West Indies. Studies in Tropical Oceanography, 5, 847.

[30] Ogden, J.C., Brown, R. a & Salesky, N. (1973) Grazing by the Echinoid Diadema antillarum Philippi: Formation of Halos around West Indian Patch Reefs. Science, 182, 715–717.

[31] Glynn, P.W. & Fong, P. (2006) Patterns of reef coral recovery by the regrowth of surviving tissues following the 1997-98 El Niño warming and 2000, 2001 upwelling cool events in Panamá, eastern Pacific. Proceedings of the 10th International Coral Reef Symposium, pp. 624–630. Okinawa.

[32] Glynn, P.W., Enochs, I.C., Afflerbach, J.A., Brandtneris, V.W. & Serafy, J.E. (2014) Eastern Pacific reef fish responses to coral recovery following El Nino disturbances. Marine Ecology

Progress Series, 495, 233–247.

[33] Copernicus - Marine environment monitoring service, https://resources.marine.copernicus.eu/?option=com_csw&task=results

[34] Solar Forecasting & Solar Irradiance Data, https://solcast.com/

[35] TIDES4FISHING, https://tides4fishing.com/as/philippines/mati-pujada-bay/

[36] Marc, C.J. (2013) Nutrient discharge from aquaculture operations in function of system design and production environment. Reviews in Aquaculture, 5, 158-171.

[37] Stadmark, J., Conley, DJ. (2011) Mussel farming as a nutrient reduction measure in the Baltic Sea: consideration of nutrient biogeochemical cycles. Marine Pollution Bulletin, 62, 1385–1388.

[38] BFAR. Bureau of Fisheries and Aquatic Resources. (2007) Managing aquaculture and its impacts: a guide book for local governments. BFAR- PHILMINAQ project, Diliman, Quezon City, 80.

[39] Ulysses, M., Bernajocele, J.S., Karl, B.S., Flordeliza, D. & Lilian C. (2020) Estimation of Nutrient Load from Aquaculture Farms in Manila Bay, Philippines. The Philippine Journal of Fisheries, 27(1), 30-39.

Acknowledgement

This research and thesis were completed during a very difficult time for anyone. I am grateful to have been able to finalize my work with the guidance and help from many people. I would like to send my most sincere thanks to them here.

First of all, I must thank my supervisor Professor Shigeru TABETA (Department of Environment Systems, Graduate School of Frontier Science at the University of Tokyo), who have always given me the greatest support and careful guidance. Whenever encountered difficulties in my research, it was his advice and guidance that gave me the greatest inspiration. My research would not have been achieved without his kind help.

Also, I would like to thank my co-supervisor, Professor Junichiro OTOMO (Department of Environment Systems) for his invaluable suggestions and comments in several discussions, which were an enormous help to me.

In addition, I must also express my gratitude to our collaborator, Professor Lea A. Jimenez (Davao Oriental State College of Science and Technology), who brought this interesting project to the table. Many of the key field data (topography, rivers, etc.) for this research were also collected and provided by their team. Many thanks for the selflessness and help.

Moreover, I would like to thank Associate Professor Katsunori MIZUNO (Department of Environment Systems). Not only during the seminars of Tabeta lab but also in the communication with the Philippine collaborators, he always gave meticulous comments and practical assistance to help me finish my thesis more easily.

Although there were some regrets during my master's education, I was able to have a great two years with the help of many friends. Shota SUZUKI, not only helped me adapt to life in Japan, but also supported me in the early stages of my research. Other members from the same laboratory including Rikito HISAMATSU, Jia WANG, Koki MIKI, Seiichiro HAGINO, Kohei KUSANO, Ziqing FENG, Yutian DING, Ruize CHEN, Shanyu CHEN, Fan ZHAO, Yuma IWATA, and Shinya SASAKI, also helped me in both studies and daily lives. I'm sure my academic life would not be as exciting without

them. Additionally, I would also like to thank the secretary in Tabeta lab, Ms. Miho HIROTANI, for her kind support and help all the time.

Finally, I would like to give my gratitude to my parents and friends who have always supported me without reservation. It is hard to imagine that I could have completed my studies and had a happy life without their encouragement and care during my overseas study life far from home.

To all the above, I would like to express my sincere thanks again. They will be my treasures forever, thanks to them.